

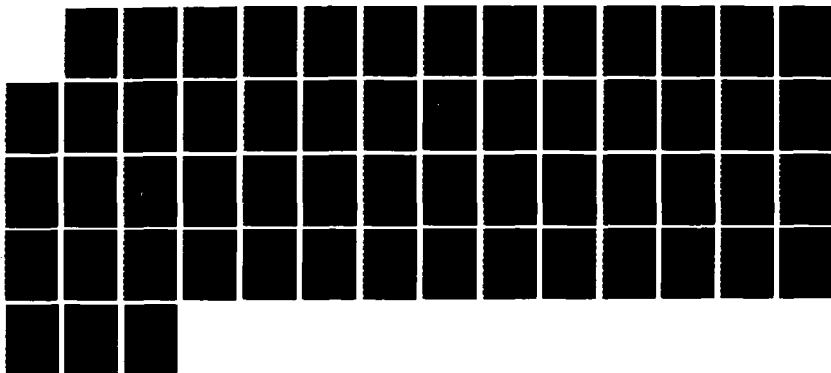
AD-A174 858

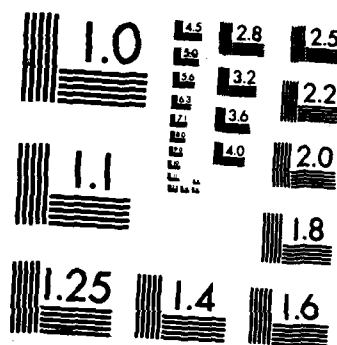
MODELING OF EQUILIBRIUM GAS ADSORPTION FOR
MULTICOMPONENT VAPOR MIXTURES PART 2(U) KENTUCKY UNIV
LEXINGTON P J REUCROFT ET AL OCT 86 CRDEC-CR-87015
DARK11-82-K-0016 F/G 7/4

1/1

UNCLASSIFIED

NL





MICROCOPY RESOLUTION TEST CHART
NATIONAL BUREAU OF STANDARDS-1963-A

AD-A174 058

CHEMICAL
RESEARCH,
— DEVELOPMENT &
ENGINEERING
CENTER

CRDEC-CR-87015

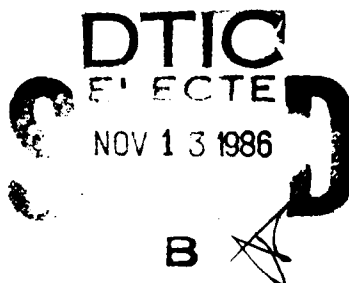
MODELING OF EQUILIBRIUM GAS
ADSORPTION FOR MULTICOMPONENT
VAPOR MIXTURES
Part II

by P. J. Reucroft
H. K. Patel
W. C. Russell
W. M. Kim

UNIVERSITY OF KENTUCKY
Lexington, KY 40506

October 1986

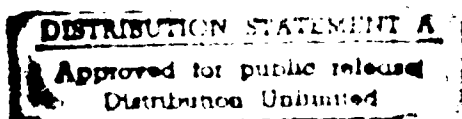
DTIC FILE COPY



U.S. ARMY
ARMAMENT
MUNITIONS
CHEMICAL COMMAND



Aberdeen Proving Ground, Maryland 21010-5423



86 11 10

Disclaimer

The findings in this report are not to be construed as an official Department of the Army position unless so designated by other authorizing documents.

Distribution Statement

Approved for public release; distribution is unlimited.

UNCLASSIFIED

SECURITY CLASSIFICATION OF THIS PAGE

AD-A174 C58

REPORT DOCUMENTATION PAGE

| | | | | | |
|---|-------|---|---|---|-----------------------------------|
| 1a. REPORT SECURITY CLASSIFICATION UNCLASSIFIED | | | 1b. RESTRICTIVE MARKINGS | | |
| 2a. SECURITY CLASSIFICATION AUTHORITY | | | 3. DISTRIBUTION/AVAILABILITY OF REPORT Approved for public release; distribution is unlimited. | | |
| 2b. DECLASSIFICATION/DOWNGRADING SCHEDULE | | | | | |
| 4. PERFORMING ORGANIZATION REPORT NUMBER(S) CRDEC-CR-87015 | | | 5. MONITORING ORGANIZATION REPORT NUMBER(S) | | |
| 6a. NAME OF PERFORMING ORGANIZATION University of Kentucky | | 6b. OFFICE SYMBOL (if applicable) | | 7a. NAME OF MONITORING ORGANIZATION | |
| 6c. ADDRESS (City, State, and ZIP Code) Lexington, KY 40506 | | | 7b. ADDRESS (City, State, and ZIP Code) | | |
| 8a. NAME OF FUNDING/SPONSORING ORGANIZATION CRDEC | | 8b. OFFICE SYMBOL (if applicable) SMCCR-RSC-A | | 9. PROCUREMENT INSTRUMENT IDENTIFICATION NUMBER DAAK11-82-K-0016 | |
| 8c. ADDRESS (City, State, and ZIP Code) Aberdeen Proving Ground, MD 21010-5423 | | | 10. SOURCE OF FUNDING NUMBERS | | |
| | | | PROGRAM ELEMENT NO. | PROJECT NO. | TASK NO. |
| | | | WORK UNIT ACCESSION NO. | | |
| 11. TITLE (Include Security Classification) Modeling of Equilibrium Gas Adsorption for Multicomponent Vapor Mixtures, Part II | | | | | |
| 12. PERSONAL AUTHOR(S) Reucroft, P. J., Patel, H. K., Russell, W. C., and Kim, W. M. | | | | | |
| 13a. TYPE OF REPORT Contractor | | 13b. TIME COVERED FROM 84 Aug TO 85 Aug | | 14. DATE OF REPORT (Year, Month, Day) 1986 October | |
| | | | | 15. PAGE COUNT 57 | |
| 16. SUPPLEMENTARY NOTATION Contracting Officer's Representative: Joseph Rehrmann, SMCCR-RSC-A, (301) 671-4297 | | | | | |
| 17. COSATI CODES | | | 18. SUBJECT TERMS (Continue on reverse if necessary and identify by block number) | | |
| FIELD | GROUP | SUB-GROUP | | | |
| 07 | 04 | | Adsorption n-Hexane CHCl ₃ | | |
| | | | Binary vapor adsorption Benzene CCl ₄ | | |
| | | | BPL-activated carbon CH ₂ Cl ₂ | | |
| 19. ABSTRACT (Continue on reverse if necessary and identify by block number) Experimental mixed vapor adsorption data on BPL-activated carbon have been obtained for several binary organic vapor mixtures and compared with the predictions of a number of multicomponent adsorption models. Mixtures include CHCl ₃ /CCl ₄ , C ₆ H ₆ /C ₆ H ₁₄ , CHCl ₃ /CH ₂ Cl ₂ and C ₆ H ₁₄ /CH ₂ Cl ₂ . Experimental techniques include an equilibrium gravimetric method and a kinetic technique which involves a study of vapor breakthrough through carbon beds. The kinetic technique yields higher values for the adsorption capacity as the polarity of the mixture increases. | | | | | |
| 20. DISTRIBUTION/AVAILABILITY OF ABSTRACT <input checked="" type="checkbox"/> UNCLASSIFIED/UNLIMITED <input type="checkbox"/> SAME AS RPT. <input type="checkbox"/> DTIC USERS | | | 21. ABSTRACT SECURITY CLASSIFICATION UNCLASSIFIED | | |
| 22a. NAME OF RESPONSIBLE INDIVIDUAL TIMOTHY E. HAMPTON | | | 22b. TELEPHONE (Include Area Code) (301) 671-2914 | | 22c. OFFICE SYMBOL SMCCR-SPS-T |

PREFACE

The work described in this report was authorized under Contract No. DAAK11-82-K-0016, Multicomponent Adsorption by Activated Carbon Adsorbents. This work was started in August 1984 and completed in August 1985.

The use of trade names or manufacturers' names in this report does not constitute an official endorsement of any commercial products. This report may not be cited for purposes of advertisement.

Reproduction of this document in whole or in part is prohibited except with permission of the Commander, U.S. Army Chemical Research, Development and Engineering Center, ATTN: SMCCR-SPS-T, Aberdeen Proving Ground, Maryland 21010-5423. However, the Defense Technical Information Center and the National Technical Information Service are authorized to reproduce the document for U.S. Government purposes.

This report has been approved for release to the public.

DTIC
ELECTE
NOV 13 1986
B

| | |
|---------------|-------------------------------------|
| Accession For | |
| NTIS | <input checked="" type="checkbox"/> |
| DTIC | <input type="checkbox"/> |
| US | <input type="checkbox"/> |
| Joint | <input type="checkbox"/> |
| By | |
| Date | |
| Auth | |
| Dist | |
| A-1 | |



CONTENTS

| | Page |
|---|------|
| 1. INTRODUCTION | 11 |
| 2. BACKGROUND | 12 |
| 2.1 Equilibrium Adsorption of Mixtures | 12 |
| 2.1.1 Dubinin-Polanyi Pore Filling Theory | 12 |
| 2.1.2 John's Mixture Isotherm Model | 14 |
| 2.1.3 Ideal Adsorbed Solution Theory | 15 |
| 2.1.4 Proportionality Method | 17 |
| 2.2 Kinetics of Adsorption | 17 |
| 3. WORK OBJECTIVES | 18 |
| 4. PROCEDURES AND RESULTS | 19 |
| 4.1 Binary Equilibrium Adsorption | 19 |
| 4.2 Results and Discussion | 19 |
| 4.3 Kinetics of Adsorption | 29 |
| 4.4 Results and Discussion | 39 |
| 5. RECOMMENDATIONS FOR FUTURE WORK | 53 |
| LITERATURE CITED | 55 |

LIST OF FIGURES

| Figure | | Page |
|--------|--|------|
| 1 | Single Vapor Adsorption Isotherms of Various Components on BPL-Activated Carbon | 20 |
| 2 | Single Vapor and Mixed Vapor Adsorption Isotherms ($\text{CCl}_4/\text{CHCl}_3$ System) on BPL-Activated Carbon | 21 |
| 3 | Experimental Mixed Vapor Isotherms ($\text{CCl}_4(20)\text{-CHCl}_3(80)$ Mixture) Compared with Theoretical Isotherms on BPL-Activated Carbon . . | 22 |
| 4 | Experimental Mixed Vapor Isotherms ($\text{CCl}_4(50)\text{-CHCl}_3(50)$ Mixture) Compared with Theoretical Isotherms on BPL-Activated Carbon . . | 23 |
| 5 | Experimental Mixed Vapor Isotherms ($\text{CCl}_4(80)\text{-CHCl}_3(20)$ Mixture) Compared with Theoretical Isotherms on BPL-Activated Carbon . . | 24 |
| 6 | Single Vapor and Mixed Vapor Isotherms ($\text{C}_6\text{H}_6\text{-C}_6\text{H}_{14}$ system) on BPL-Activated Carbon | 25 |
| 7 | Experimental Mixed Vapor Isotherms ($\text{C}_6\text{H}_6(25)\text{-C}_6\text{H}_{14}(75)$ Mixture) Compared with Theoretical Isotherms on BPL-Activated Carbon . . | 26 |
| 8 | Experimental Mixed Vapor Isotherms ($\text{C}_6\text{H}_6(50)\text{-C}_6\text{H}_{14}(50)$ Mixture) Compared with Theoretical Isotherms on BPL-Activated Carbon . . | 27 |
| 9 | Experimental Mixed Vapor Isotherms ($\text{C}_6\text{H}_6(25)\text{-C}_6\text{H}_{14}(75)$ Mixture) Compared with Theoretical Isotherms on BPL-Activated Carbon | 28 |
| 10 | Single Vapor and Mixed Vapor Isotherms ($\text{C}_6\text{H}_{14}\text{-CH}_2\text{Cl}_2$ system) on BPL-Activated Carbon | 30 |
| 11 | Experimental Mixed Vapor Isotherms ($\text{C}_6\text{H}_{14}(90)\text{-CH}_2\text{Cl}_2(10)$ Mixture) Compared with Theoretical Isotherms on BPL-Activated Carbon . . | 31 |
| 12 | Experimental Mixed Vapor Isotherms ($\text{C}_6\text{H}_{14}(75)\text{-CH}_2\text{Cl}_2(25)$ Mixture) Compared with Theoretical Isotherms on BPL-Activated Carbon . . | 32 |
| 13 | Experimental Mixed Vapor Isotherms ($\text{C}_6\text{H}_{14}(50)\text{-CH}_2\text{Cl}_2(50)$ Mixture) Compared with Theoretical Isotherms on BPL-Activated Carbon . . | 33 |
| 14 | Experimental Mixed Vapor Isotherms ($\text{C}_6\text{H}_{14}(25)\text{-CH}_2\text{Cl}_2(75)$ Mixture) Compared with Theoretical Isotherms on BPL-Activated Carbon . . | 34 |
| 15 | Single Vapor and Mixed Vapor Isotherms ($\text{CHCl}_3\text{-CH}_2\text{Cl}_2$ System) on BPL-Activated Carbon | 35 |
| 16 | Experimental Mixed Vapor Isotherms ($\text{CHCl}_3(80)\text{-CH}_2\text{Cl}_2(20)$ Mixture) Compared with Theoretical Isotherms on BPL-Activated Carbon . . | 36 |
| 17 | Experimental Mixed Vapor Isotherms ($\text{CHCl}_3(50)\text{-CH}_2\text{Cl}_2(50)$ Mixture) Compared with Theoretical Isotherms on BPL-Activated Carbon . . | 37 |

| | | |
|----|--|----|
| 18 | Experimental Mixed Vapor Isotherms (CHCl_3 (20)- CH_2Cl_2 (80) Mixture) Compared with Theoretical Isotherms on BPL-Activated Carbon . . | 38 |
| 19 | Vapor-Adsorbed Phase Equilibria for n-Hexane/Benzene Binary Mixture (BPL-Activated Carbon, $T = 25^\circ\text{C}$, $P_T = 25$ torr, flow rate = $400\text{ cm}^3/\text{min.}$) | 41 |
| 20 | Vapor-Adsorbed Phase Equilibria for $\text{CHCl}_3/\text{CH}_2\text{Cl}_2$ Binary Mixture (BPL-Activated Carbon, $T = 25^\circ\text{C}$, $P_T = 25$ torr, flow rate = $400\text{ cm}^3/\text{min.}$) | 42 |
| 21 | Vapor-Adsorbed Phase Equilibria for n-Hexane/ CH_2Cl_2 Binary Mixture (BPL-Activated Carbon, $T = 25^\circ\text{C}$, $P_T = 25$ torr, flow rate = $400\text{ cm}^3/\text{min.}$) | 43 |

LIST OF TABLES

| Table | | Page |
|-------|---|------|
| 1 | Breakthrough Time (t_b) as a Function of Bed Weight (W_b) for the CH_2Cl_2 /n-Hexane Binary System on BPL-Activated Carbon. (Flow Rate = $400 \text{ cm}^3/\text{min.}$, $P_T = 25 \text{ torr}$, $T = 298^\circ\text{K}$) | 40 |
| 2 | Breakthrough Time, t_b , as a Function of Composition and Bed Weight (W_b) for n-Hexane/Benzene Binary Mixtures . . | 44 |
| 3 | Kinetic Saturation Capacities (W_e), Direct Weight Saturation Capacities (W_m) and Equilibrium Capacities (W_g) for the CH_2Cl_2 /n-Hexane Binary System on BPL-Activated Carbon. (Flow rate = $400 \text{ cm}^3/\text{min.}$, $P_T = 25 \text{ torr}$, $T = 298^\circ\text{K}$) | 45 |
| 4 | Kinetic Saturation Capacities (W_e), Direct Weight Saturation Capacities (W_m) and Equilibrium Capacities (W_g) for the C_6H_6 /n-Hexane Binary System on BPL-Activated Carbon (Flow rate = $400 \text{ cm}^3/\text{min.}$, $P_T = 25 \text{ torr}$, $T = 298^\circ\text{K}$). | 45 |
| 5 | Comparison of Adsorption Capacities Obtained from Several Predictive Models with the Experimental Values (W_e & W_g) for the Benzene/n-Hexane Mixture ($P_T = 25 \text{ torr}$, flow rate = $400 \text{ cm}^3/\text{min}$) | 46 |
| 6 | Comparison of Adsorption Capacities Obtained from Several Predictive Models with the Experimental Values (W_e & W_g) for the $\text{CHCl}_3/\text{CCl}_4$ Mixture ($P_T = 25 \text{ torr}$, flow rate = $400 \text{ cm}^3/\text{min}$) | 47 |
| 7 | Comparison of Adsorption Capacities Obtained from Several Predictive Models with that of Experimental Capacities (W_e & W_g) for the $\text{CHCl}_3/\text{CH}_2\text{Cl}_2$ Mixture ($P_T = 25 \text{ torr}$, flow rate = $400 \text{ cm}^3/\text{min}$) | 48 |
| 8 | Comparison of Adsorption Capacities Obtained from Several Predictive Models with the Experimental Values (W_e & W_g) for the CH_2Cl_2 /n-Hexane Mixture ($P_T = 25 \text{ torr}$, flow rate = $400 \text{ cm}^3/\text{min}$) | 49 |
| 9 | Affinity Coefficient Difference and Saturated Vapor Pressure Difference of Components in Mixtures Investigated . . . | 49 |
| 10 | Calculated Capacities (Methods 1 and 2) and Experimental Kinetic Capacities (W_e) for the n-Hexane/Benzene Mixture on BPL-Activated Carbon ($P_T = 25 \text{ torr}$ and flow rate of $400 \text{ cm}^3/\text{min}$) | 50 |

| | | |
|----|---|----|
| 11 | Calculated Capacities (Methods 1 and 2) and Experimental Kinetic Capacities (W_e) for the $\text{CH}_2\text{Cl}_2/\text{CHCl}_3$ Mixture on BPL-Activated Carbon ($P_T = 25$ torr and flow rate of $400 \text{ cm}^3/\text{min}$) | 51 |
| 12 | Calculated Capacities (Methods 1 and 2) and Experimental Kinetic Capacities (W_e) for the n-Hexane/ CH_2Cl_2 Mixture on BPL-Activated Carbon ($P_T = 25$ torr and flow rate of $400 \text{ cm}^3/\text{min}$) | 52 |

MODELING OF EQUILIBRIUM GAS ADSORPTION FOR
MULTICOMPONENT VAPOR MIXTURES
PART II

1. INTRODUCTION

Single vapor equilibrium adsorption isotherms are often used to assess the relative efficiencies with which adsorbents, such as activated carbon, remove specific vapors from air in air purification schemes. Single vapor adsorption isotherms can often be predicted at equilibrium, subject to some limitations, from the physical properties of the adsorbate vapors by techniques based upon the Dubinin-Polanyi concept of affinity coefficient.¹⁻⁴ Past studies have provided vast amounts of adsorption isotherm data for single vapor adsorption on various adsorbents. However, the practical conditions under which adsorbents are employed are usually quite different from the ideal laboratory conditions under which the single vapor isotherms are determined. For example, several adsorbate species are usually present. The vapor species to be adsorbed may not be exposed to the adsorbent under conditions where equilibrium can be readily attained. The study of multicomponent kinetic and equilibrium adsorption on an adsorbent is very important; however, kinetic and equilibrium adsorption studies are still at a very preliminary stage while mixed vapor adsorption studies are more complex and time consuming. This problem can be alleviated to some extent if mixed adsorption isotherms can be predicted from single vapor adsorption data.

Although there has been considerable study involving the thermodynamic properties of adsorbates on adsorbents, relatively few studies have considered adsorption kinetics. Most of the studies to date⁵⁻⁷ have dealt with the kinetics of single vapor adsorption behavior. Many of these studies have made use of Wheeler's approach to the kinetics of gas adsorption by beds of

adsorbent granules. This method has yet to be successfully applied to multicomponent systems.

The development of experimental methods for determining binary adsorption isotherms and the kinetics of binary mixture adsorption was completed in the first year of the project. In the second year, the adsorption of $\text{CHCl}_3/\text{CCl}_4$, n-Hexane/Benzene, and $\text{CH}_2\text{Cl}_2/\text{CHCl}_3$ binary systems on BPL-activated carbon was investigated. BPL is a designation assigned by Calgon Corporation. In the past year, additional equilibrium and kinetic adsorption studies were carried out on n-hexane/benzene, $\text{CH}_2\text{Cl}_2/\text{CHCl}_3$ and n-hexane/ CH_2Cl_2 binary mixtures. Also, potentially useful theoretical models were applied to all the binary systems studied during the reporting period. Results and conclusions from these studies are presented in addition to the recommendations for work to be carried out in the future.

2. BACKGROUND

2.1 Equilibrium Adsorption of Mixtures.

Currently, there are four potentially useful theoretical methods available which have had limited success in predicting the adsorption characteristics of mixtures:

- a. Dubinin-Polanyi Pore Filling Theory¹
- b. John's mixture isotherm model⁸
- c. Myer's ideal adsorption solution theory⁹
- d. Proportionality Method¹⁰

2.1.1 Dubinin-Polanyi Pore Filling Theory.

The Dubinin-Polanyi theory has not been used much to predict multicomponent adsorption. The results that are available indicate, however, that the theory has some potential for application to multicomponent adsorption. Bering and co-workers^{11,12} extended the Dubinin-Polanyi equation to the adsorption of mixtures by using the following equation:

$$\Sigma a_i = \frac{W_o}{\Sigma N_i \bar{v}_i} \exp \left[-BT^2 \left(\frac{\Sigma N_i \log(p_{si}/p_i)}{(\Sigma N_i \bar{\beta}_i)} \right)^2 \right] \quad (1)$$

where \bar{v}_i = the partial molar volume of mixture component i

$\bar{\beta}_i$ = the partial molar affinity coefficient of mixture component i

p_{si} = the saturated vapor pressure of mixture component i

p_i = the equilibrium pressure of mixture component i

a_i = the number of g mole of component i adsorbed per gm of adsorbent

N_i = the mole fraction of component i in the adsorbed phase

W_o and B = constants characterizing the adsorbent

In practice, the quantity $\Sigma N_i \bar{v}_i$ can be found from the phase diagram of the volume solution assuming a liquid-like adsorbate, while $\Sigma N_i \bar{\beta}_i$ can be found simply according to an additive scheme.¹³

In the theory of micropore filling in the case of an individual component, a normal liquid at the given temperature, existing in equilibrium with its saturated vapor at the pressure, P_o , is selected as the standard state. In the case of multicomponent adsorption, it is unclear, a priori, whether the state of a solution whose composition is equal to the composition of the adsorbed phase or the state of a solution existing in equilibrium with vapor whose composition is equal to the composition of the equilibrium vapor above the adsorbed phase should be selected as the standard state. However, studies¹² have shown that Equation (1) is fulfilled well in both methods of selecting the standard state. Selecting such standard states, we can rewrite Equation (1) for a binary mixture of vapors in the following form:

$$W = a_{12} v_{12} = W_o \exp \left[\frac{-BT^2}{\beta_{12}} \left(\log \left(\frac{1}{h} \right) \right)^2 \right] \quad (2)$$

where

$$h = \frac{\sum p_i}{\sum p_{si}} = \frac{p_1}{p_{s1}} = \frac{p_2}{p_{s2}}$$

Equation (2) was found to be applicable to several systems.¹⁴ Other methods based on the Dubinin-Polanyi approach have also been described in literature.^{15,16}

2.1.2 John's Mixture Isotherm Model.

This model, which was developed by John and others,⁸ assumes that the single vapor isotherms for species i can be represented by the following equation:

$$\log \log P_i^o = C_i + D_i \log W_i^o \quad (3)$$

where C_i = a constant

D_i = a constant

W_i^o = amount of adsorbate in cm^3/g at pressure, p_i

$P_i^o = (p_i/p_{s1}) 10^N$

and superscript 'o' denotes pure component. N is an integer between 2 and 6.

A similar equation describes the binary vapor (components 1 and 2) adsorption isotherm:

$$\log \log P_{12} = C_{12} + D_{12} \log W_{12} \quad (4)$$

where $C_{12} = Y_1 C_1 + Y_2 C_2$

$D_{12} = Y_1 D_1 + Y_2 D_2$

W_{12} = the amount of mixed adsorbate

$P_{12} = (p_1 + p_2)/(p_{s1} + p_{s2}) 10^N$

and Y_1 and Y_2 are the mole fractions of components 1 and 2 in the gas phase.

The constants C_1 , C_2 , D_1 , and D_2 can be obtained from the single vapor isotherms and then used to calculate W_{12} , in Equation (4), using known or assumed P_{12} values.

From the model, the micropore volume, W_0 , can be computed for a single vapor component 1 as follows:

$$\log W_0 = (\log \log 10^N - C_1)/D_1 \quad (5)$$

Similarly the micropore volume in the binary mixture case is given by:

$$\log W_0 = (\log \log 10^N - C_{12})/D_{12} \quad (6)$$

John and others⁸ have shown that this method can be applied to binary and ternary systems to compute their total adsorption.

2.1.3 Ideal Adsorbed Solution Theory.

The ideal adsorbed solution theory has been used to predict mixed gas adsorption with some success at low coverages/low relative pressure.^{9,17} The method assumes that the adsorbed phase forms an ideal solution and involves determining the 'spreading pressure' for the single vapor isotherms. The calculation is made as follows:

- a. Obtain the single vapor isotherms for pure components in terms of the amount absorbed, (cc/g) versus equilibrium pressure (torr).
- b. The spreading pressure for these adsorbates is calculated as follows:

$$\frac{\pi A}{RT} = \int_0^P \frac{n}{p_1^0} dp_1^0 \quad (7)$$

where π = spreading pressure

A = specific area of adsorbent

n = total number of moles in adsorbed phase/gm of adsorbent

p_1^0 = equilibrium vapor pressure of pure component

c. Calculate the vapor pressure of pure components at constant spreading pressure.

d. Describe the amount adsorbed (n_1^o) at these vapor pressures (calculated in step c) from step a.

e. Calculate the adsorption equilibria for both components at a desired total pressure, P, using the following two equations:

$$Py_1 = p_1^o N_1 \quad (8)$$

$$Py_2 = p_2^o N_2 \quad (9)$$

Adding these two equations, the expression for an ideal liquid solution is obtained.

$$N_1 = \frac{P - p_2^o}{p_1^o - p_2^o} \quad (10)$$

The vapor phase composition is given by:

$$Y_1 = \frac{p_1^o N_1}{P} \quad (11)$$

N_1 is the mole fraction of component 1 in the adsorbed phase and Y_1 is the mole fraction of component 1 in the gas phase.

f. The total amount adsorbed is obtained by:

$$\frac{1}{n} = \sum \frac{N_i}{n_i^o} \quad (12)$$

g. Finally, the amount of each component adsorbed from the gas mixture is given by: $n_i = nN_i$.

The complete isobaric composition diagram for any mixture is obtained by repeating the above calculation for different values of the spreading pressure.

2.1.4 Proportionality Method.

Recently Jonas, et al.¹⁰ suggested that the adsorption behavior of a mixture can successfully be predicted using a simple technique called the proportionality method. In this technique vapor concentrations are expressed in terms of their mole fractions. The equation can be written as follows:

$$W_{12} = Y_1 W_1 + Y_2 W_2 \quad (13)$$

where W_{12} = amount of mixed adsorbate (g/g)

W_1 = the amount adsorbed of component 1 from the single vapor (g/g)

W_2 = the amount adsorbed of component 2 from the single vapor (g/g)

Y_1 = mole fraction of component 1 in the gas phase of a mixture

Y_2 = mole fraction of component 2 in the gas phase of a mixture

Jonas, et al.¹⁰ have applied this method to binary systems with some degree of success.

2.2 Kinetics of Adsorption.

Studies on the kinetics of adsorption on activated carbon have been previously reported⁵⁻⁷ for the case of single vapor adsorption but have yet to be extended to multicomponent mixtures. However, many of the mathematical equations and kinetic processes which describe these phenomena for single vapors should also be applicable to multicomponent mixtures. Of particular interest is the approach taken by Wheeler^{18,19} which has been used successfully for single vapor adsorption kinetics.⁵⁻⁷ Wheeler's equation, which is based on the principle of mass conservation, can be written as follows:

$$t_b = (W_e/C_o Q) [W_b - \rho_B Q \ln(C_o/C_x)/k_v] \quad (14)$$

where C_o = the inlet gas concentration in g/cm³

k_v = the first order rate constant in min⁻¹

ρ_B = the bulk density of packing in g/cm³
 W_e = the kinetic saturation capacity in g/g
 W_b = the bed weight in gm
 Q = the volume flow rate in cm³/min
 t_b = the breakthrough time in min
 C_x = the exit gas concentration.

From a plot of t_b versus W_b , the saturation capacity (W_e) and the first order rate constant (k_v) can be obtained. By setting t_b of Equation (13) equal to zero and solving for W_b one obtains

$$W_b = \rho_B Q / k_v \ln (C_0 / C_x) = W_C \quad (15)$$

where W_C is identified as the critical bed weight, or that weight of carbon just sufficient to reduce C_0 to C_x under the test conditions.

3. WORK OBJECTIVES

The ultimate objectives of the study are to develop methods for predicting the adsorptive behavior of mixed gas systems on activated carbon adsorbents from a knowledge of the adsorptive properties of the pure components and to determine applicability of the Wheeler equation to multi-component kinetic adsorption.

The work has been divided into the following four phases: (1) determination of equilibrium adsorption isotherms on BPL-activated carbon for various binary vapor mixtures at 25°C, (2) prediction of binary vapor adsorption isotherms on BPL-activated carbon for comparison with experimentally determined isotherms, (3) determination of breakthrough parameters through adsorbent beds for single vapors and binary vapor mixtures, and (4) testing the applicability of Wheeler's equation to binary systems.

Another objective has been to investigate the effect of adsorbate polarity on the predictive techniques and, also, the effect of adsorbate polarity on the mixed vapor adsorption data obtained through the use of Wheeler's equation. The mixtures investigated experimentally to date contained (i) two non-polar components (NP-NP), (ii) two weakly polar components (WP-WP) and (iii) a non-polar component and a weakly polar component (NP-WP).

4. PROCEDURES AND RESULTS

4.1 Binary Equilibrium Adsorption.

The apparatus and experimental procedures used for measuring the single and binary vapor adsorption isotherms have been described in a previous report by Reucroft and others.²⁰

The activated carbon was a Pittsburgh-activated carbon, type BPL, 12-30 mesh, having an internal surface area of about 1000 m²/g and approximately 80% of the internal surface area associated with pores less than 20 Å in diameter.

The experimental procedure (Method B) used in the equilibrium studies of mixed vapors has been previously described.²¹

4.2 Results and Discussion.

Figure 1 shows the single vapor adsorption isotherms for various vapors on BPL activated carbon at room temperature in terms of amount adsorbed (gm/gm of activated carbon) versus equilibrium vapor pressure.

Figures 2-5 show the experimental single and mixed vapor adsorption isotherms of the CCl₄-CHCl₃ binary system and comparison of experimental and theoretical adsorption isotherm data. The theoretical adsorption capacities were calculated using D-P theory and John's equation. Agreement between the predicted and experimental equilibrium capacities is quite good. Therefore,

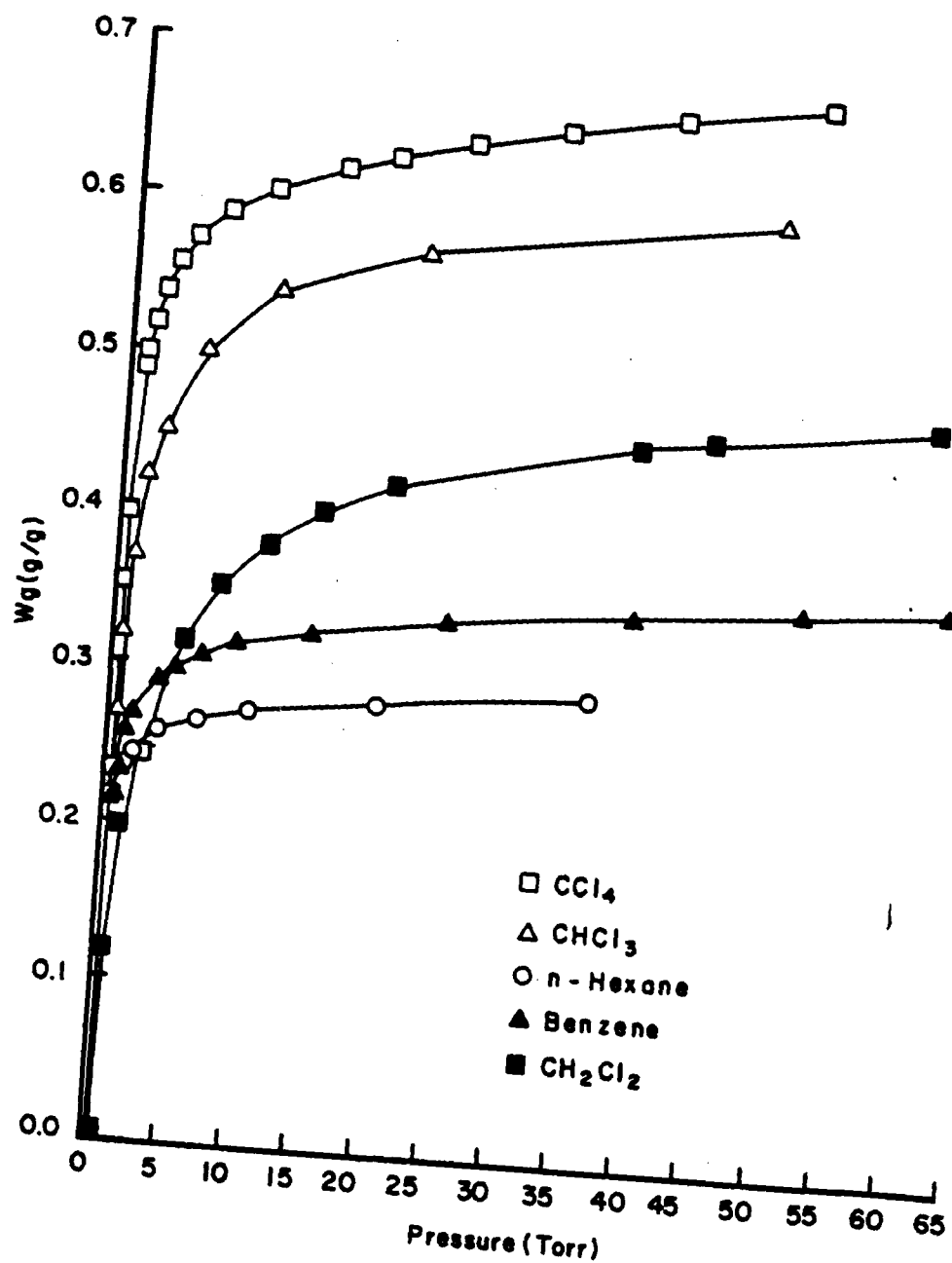


Figure 1. Single Vapor Adsorption Isotherms of Various Components on BPL-Activated Carbon

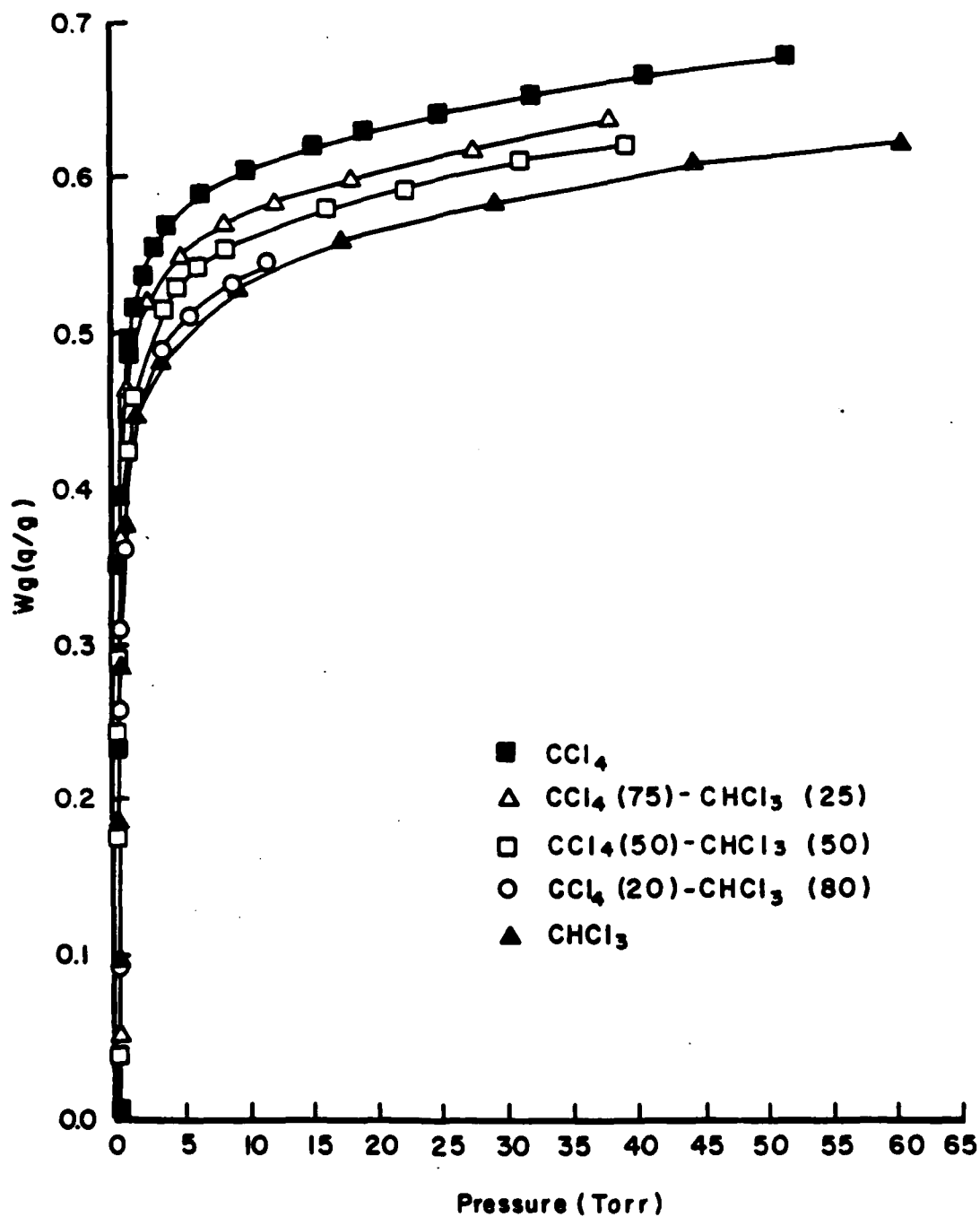


Figure 2. Single Vapor and Mixed Vapor Adsorption Isotherms (CCl_4 - CHCl_3 System) on BPL-Activated Carbon

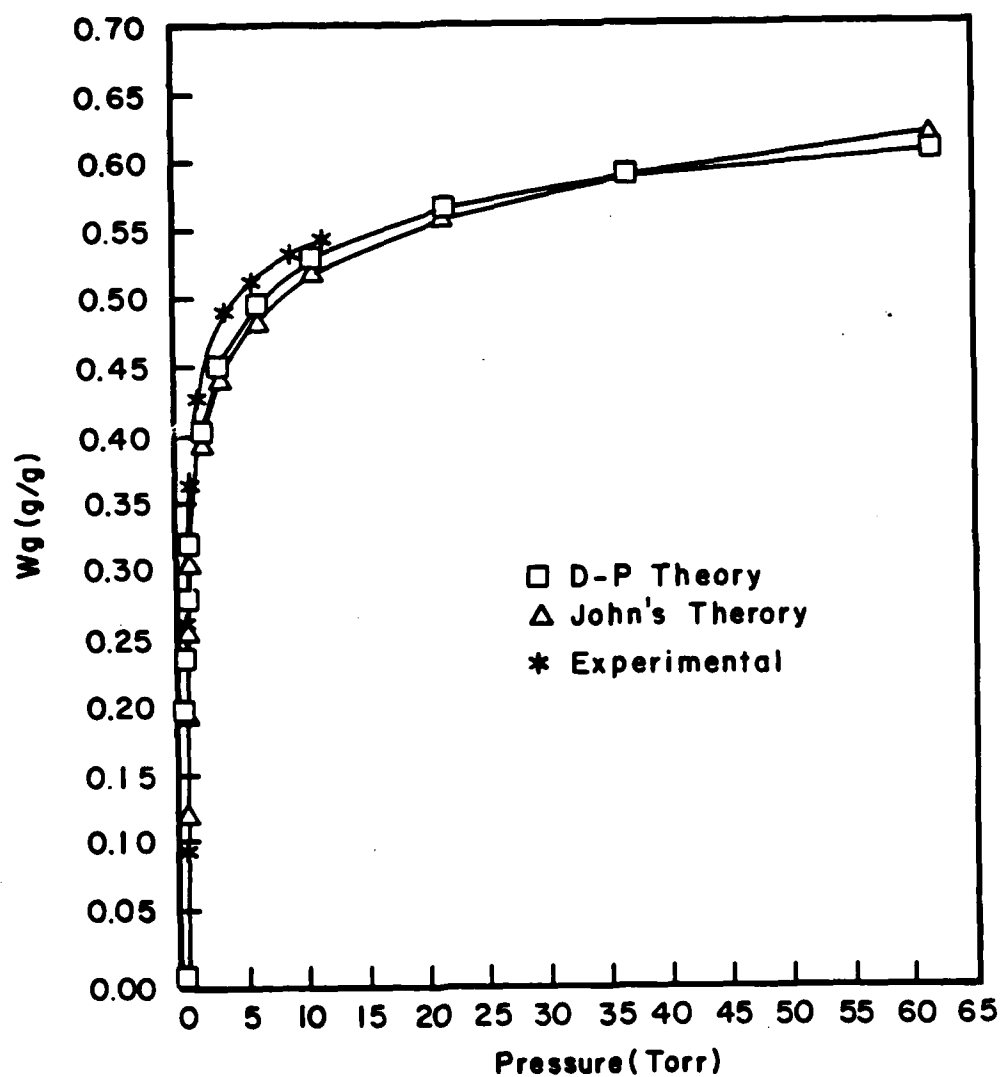


Figure 3. Experimental Mixed Vapor Isotherms ($\text{CCl}_4(20)\text{-CHCl}_3(80)$ Mixture) Compared with Theoretical Isotherms on ^4BPL -Activated Carbon

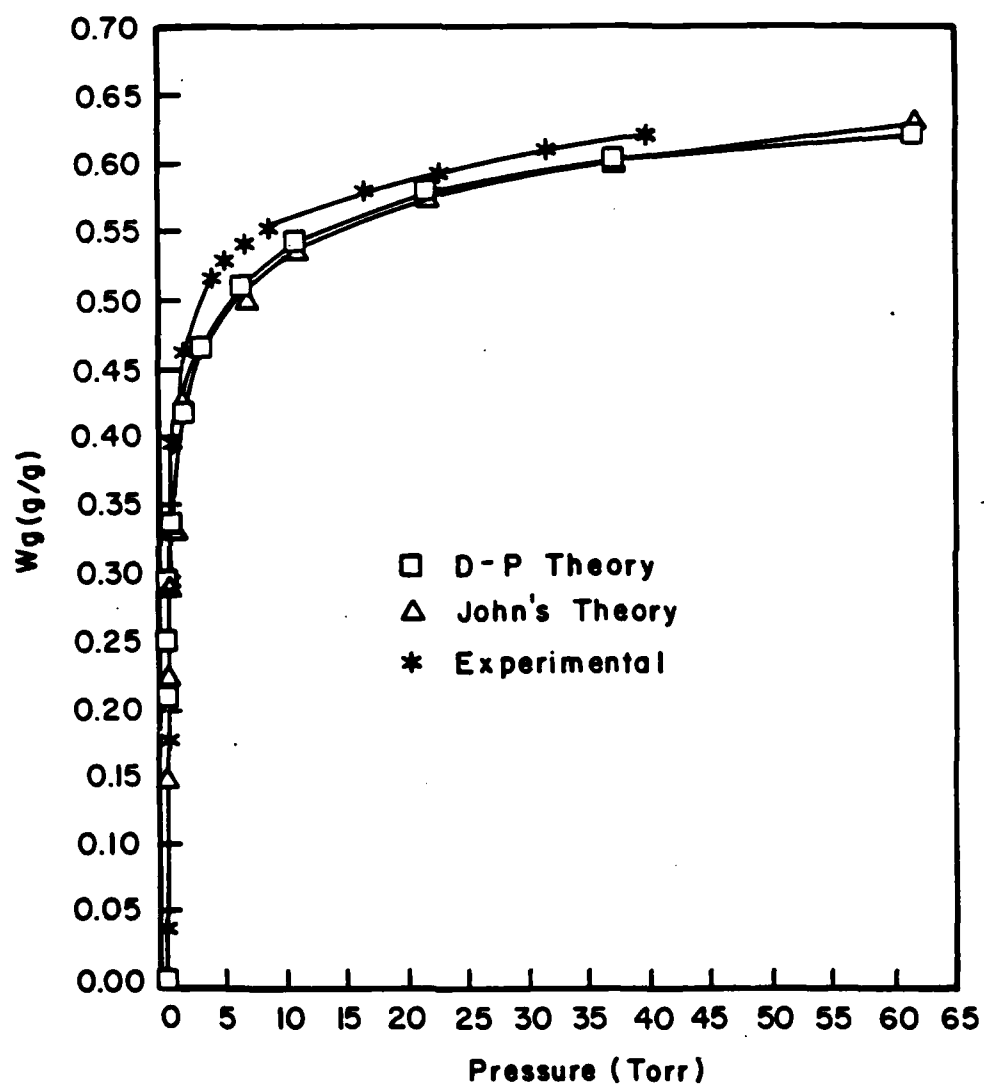


Figure 4. Experimental Mixed Vapor Isotherms ($\text{CCl}_4(50)\text{-CHCl}_3(50)$ Mixture) Compared with Theoretical Isotherms on BPL-Activated Carbon

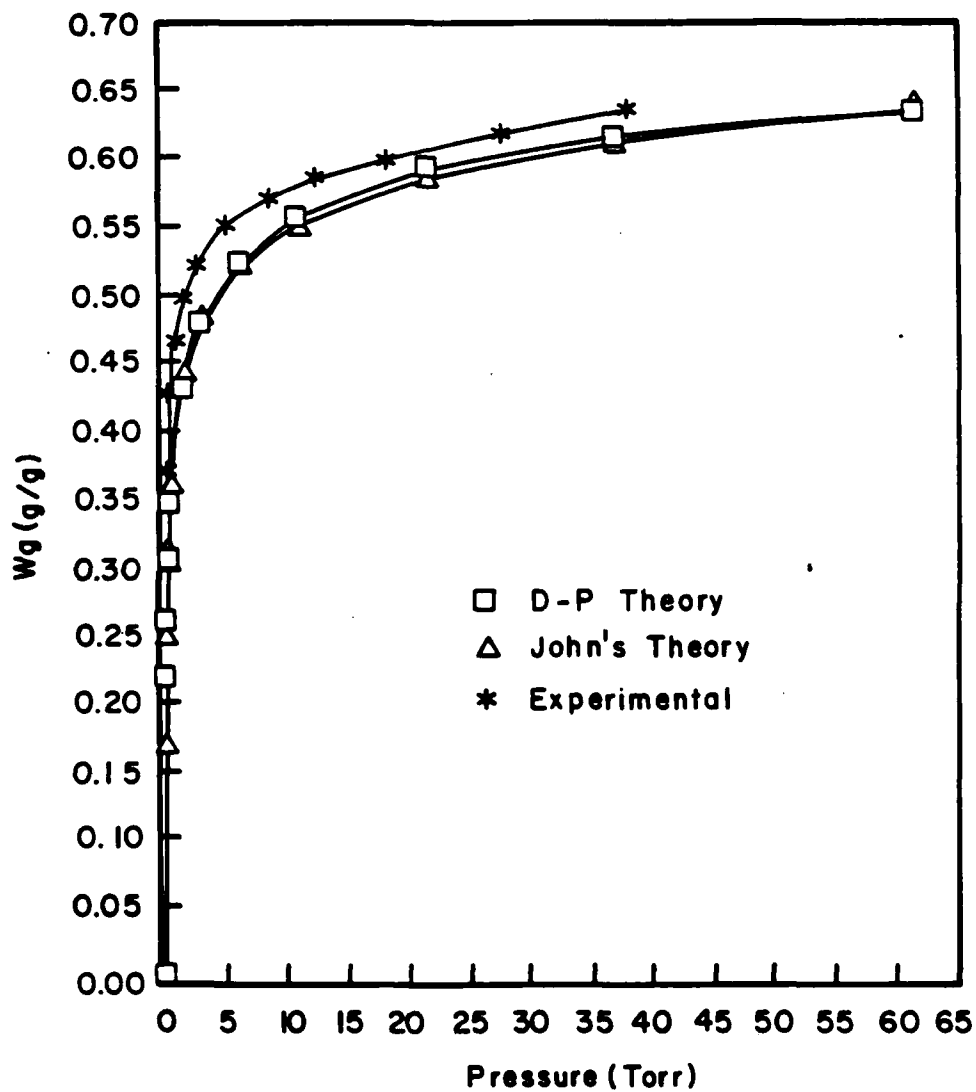


Figure 5. Experimental Mixed Vapor Isotherms ($\text{CCl}_4(80)\text{-CHCl}_3(20)$ Mixture) Compared with Theoretical Isotherms on BPL-Activated Carbon

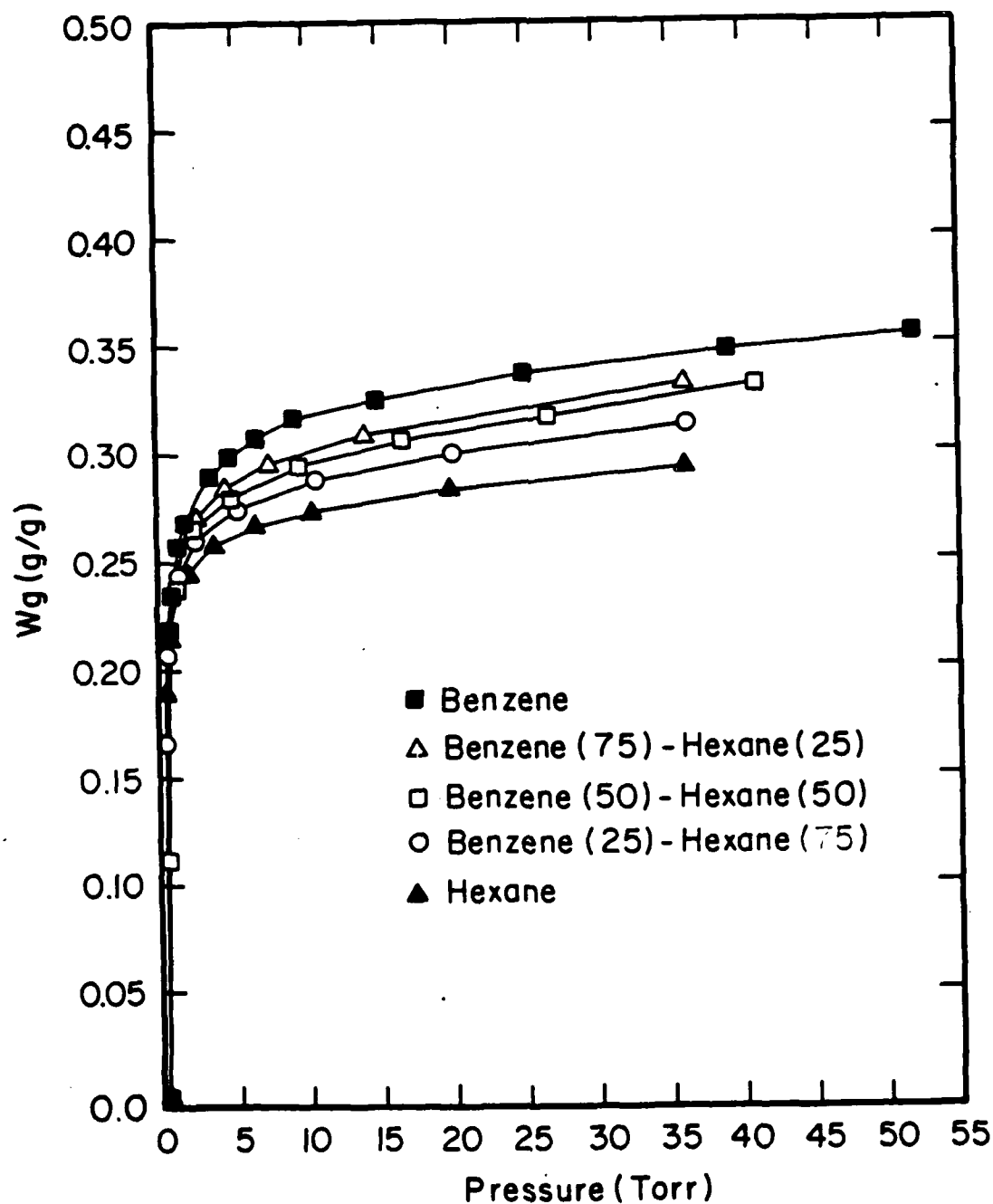


Figure 6. Single Vapor and Mixed Vapor Isotherms (C_6H_6 - C_6H_{14} System) on BPL-Activated Carbon

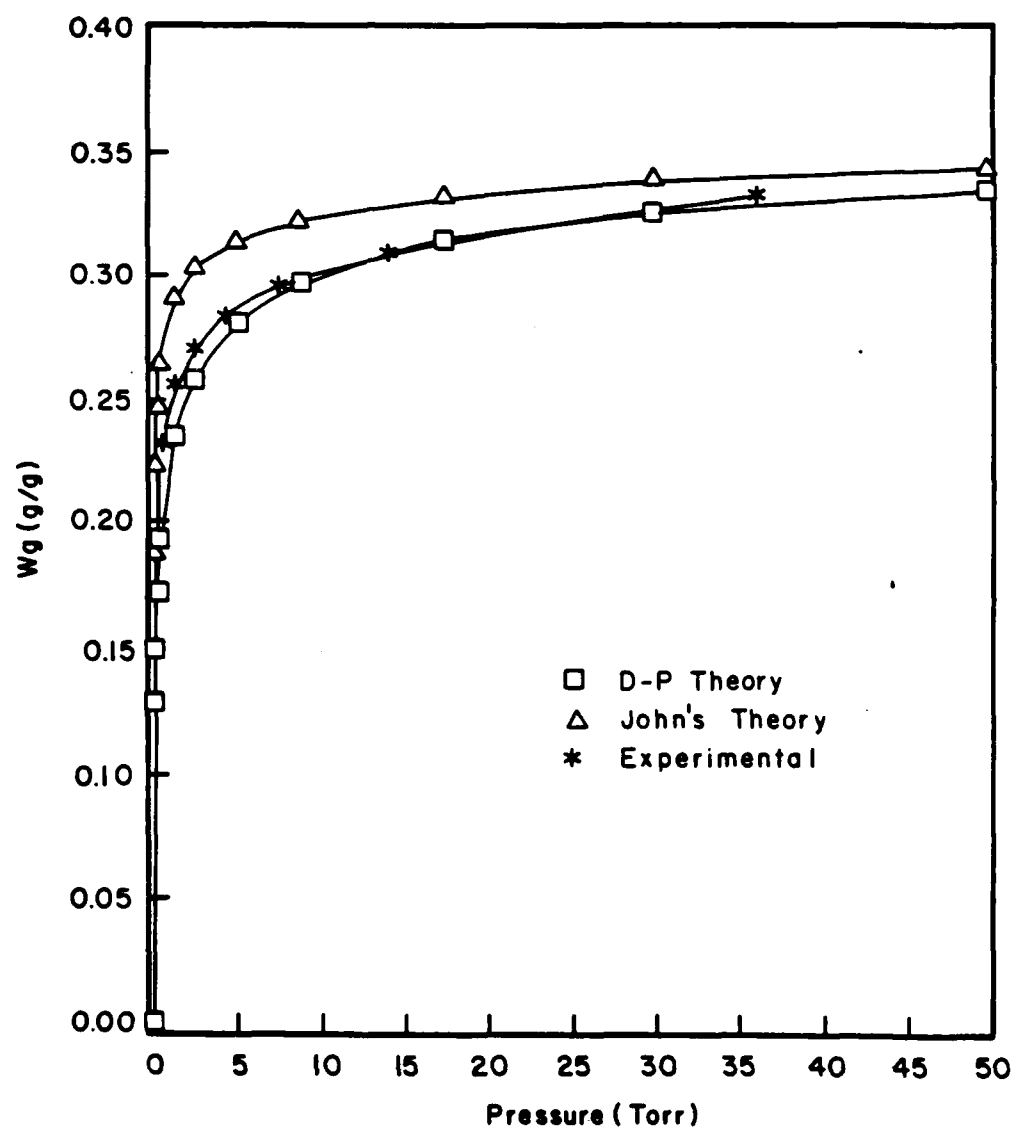


Figure 7. Experimental Mixed Vapor Isotherms ($C_6H_6(25)-C_6H_{14}(75)$ Mixture) Compared with Theoretical Isotherms on BPL-Activated Carbon

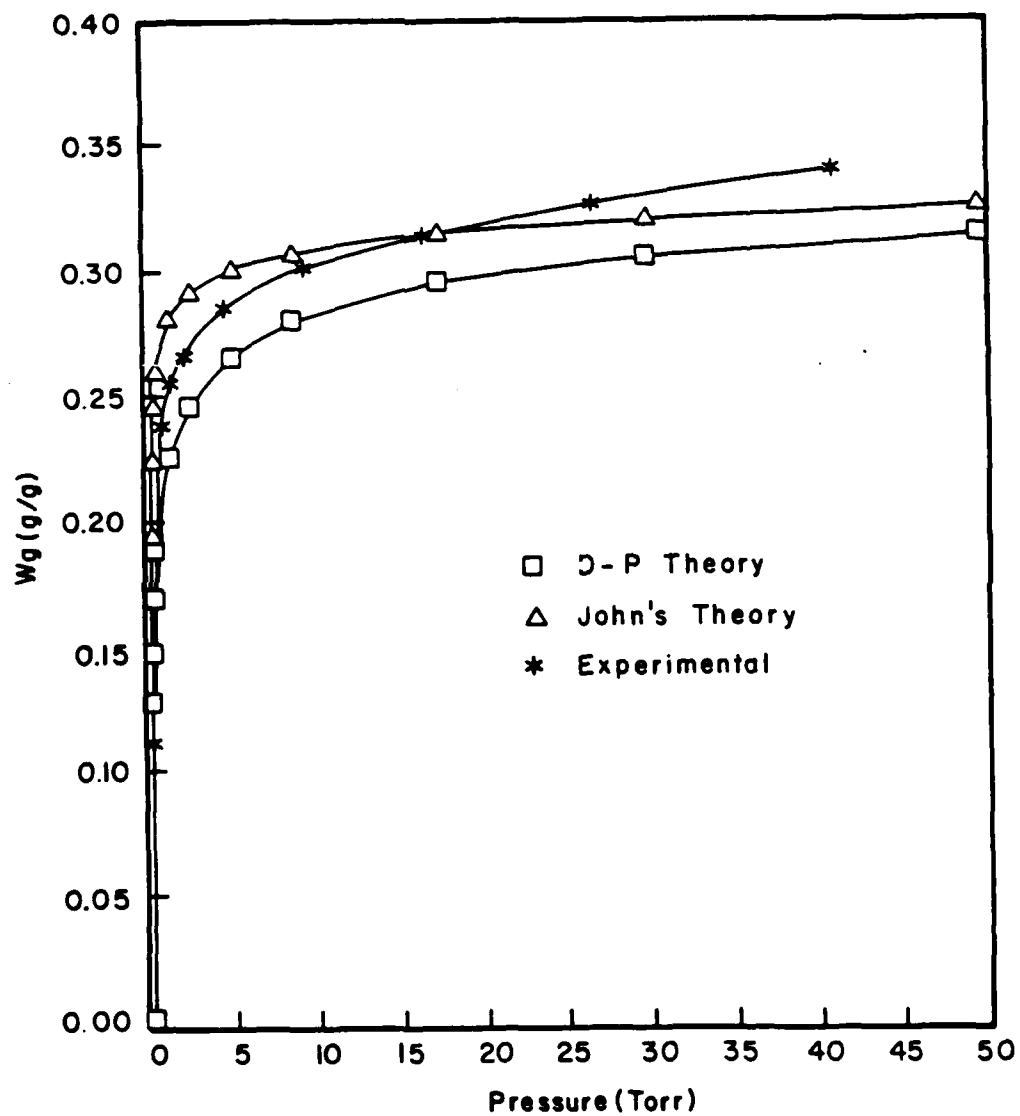


Figure 8. Experimental Mixed Vapor Isotherms ($C_6H_6(50)-C_6H_{14}(50)$ Mixture) Compared with Theoretical Isotherms on BPL-Activated Carbon

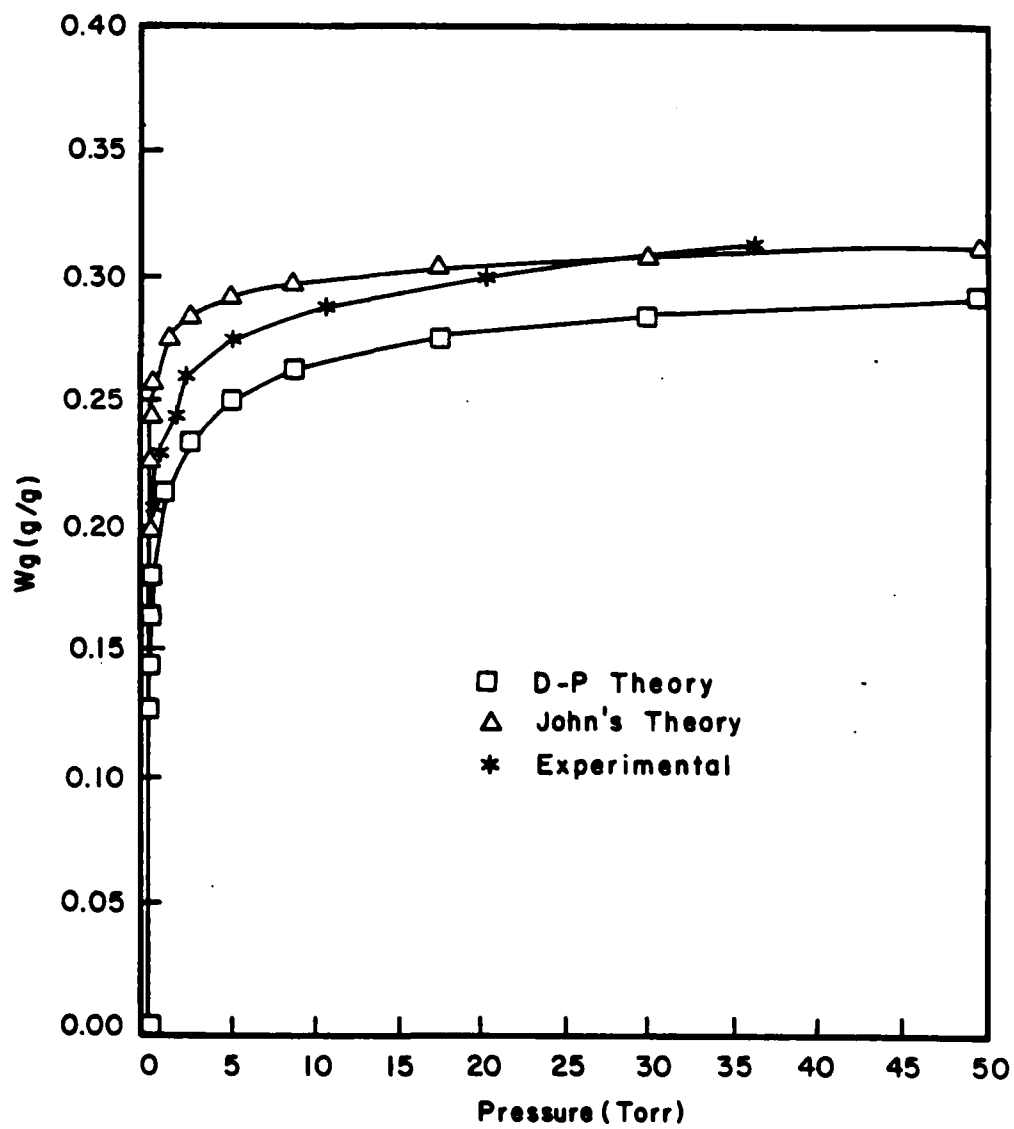


Figure 9. Experimental Mixed Vapor Isotherms ($C_6H_6(25)-C_6H_{14}(75)$ Mixture) Compared with Theoretical Isotherms on BPL-Activated Carbon

either D-P theory or John's equation can be used to calculate adsorption capacity of $\text{CHCl}_3/\text{CCl}_4$ mixtures. Experimental isotherms for the n-hexane/benzene system are shown in Figure 6. Experimental and theoretical isotherms are compared in Figures 7 to 9 for this system. Similar results are shown for the n-hexane/ CH_2Cl_2 system in Figures 10 to 14, and for the $\text{CHCl}_3/\text{CH}_2\text{Cl}_2$ system in Figures 15 to 18.

In the case of the n-hexane/benzene system, the experimental isotherm agrees well with John's isotherm equation for two mixtures. Better agreement is obtained with the DP theory in the case of the $\text{C}_6\text{H}_6(25)\text{-C}_6\text{H}_{14}(75)$ Mixture.

The mixture isotherms are very similar to the n-hexane isotherms for all the mixtures investigated in the case of the n-hexane/ CH_2Cl_2 system. The experimental isotherms do not agree well with either of the two models for this system.

In the case of the $\text{CHCl}_3/\text{CH}_2\text{Cl}_2$ system, both theoretical models tend to underestimate the adsorption amount over the pressure range investigated.

4.3 Kinetics of Adsorption.

The experimental procedure and a schematic of the binary vapor test apparatus used for determining the kinetics of adsorption were described in an earlier report by Reucroft, et al.²⁰ The concentration of each component was determined from the traced area of the gas chromatograph peak. The ratio of the exit concentration, C_x , to the inlet concentration, C_0 , was plotted as a function of time, t . This is the time when concentration ratio reaches 0.01 ($C_x/C_0 = 0.01$) is called breakthrough time, t_b . A linear regression analysis of the data for t_b (breakthrough time) vs W_b (carbon bed weight) for a binary mixture yielded W_e values for individual components from Wheeler's equation. Total adsorption of the bed, W_m was

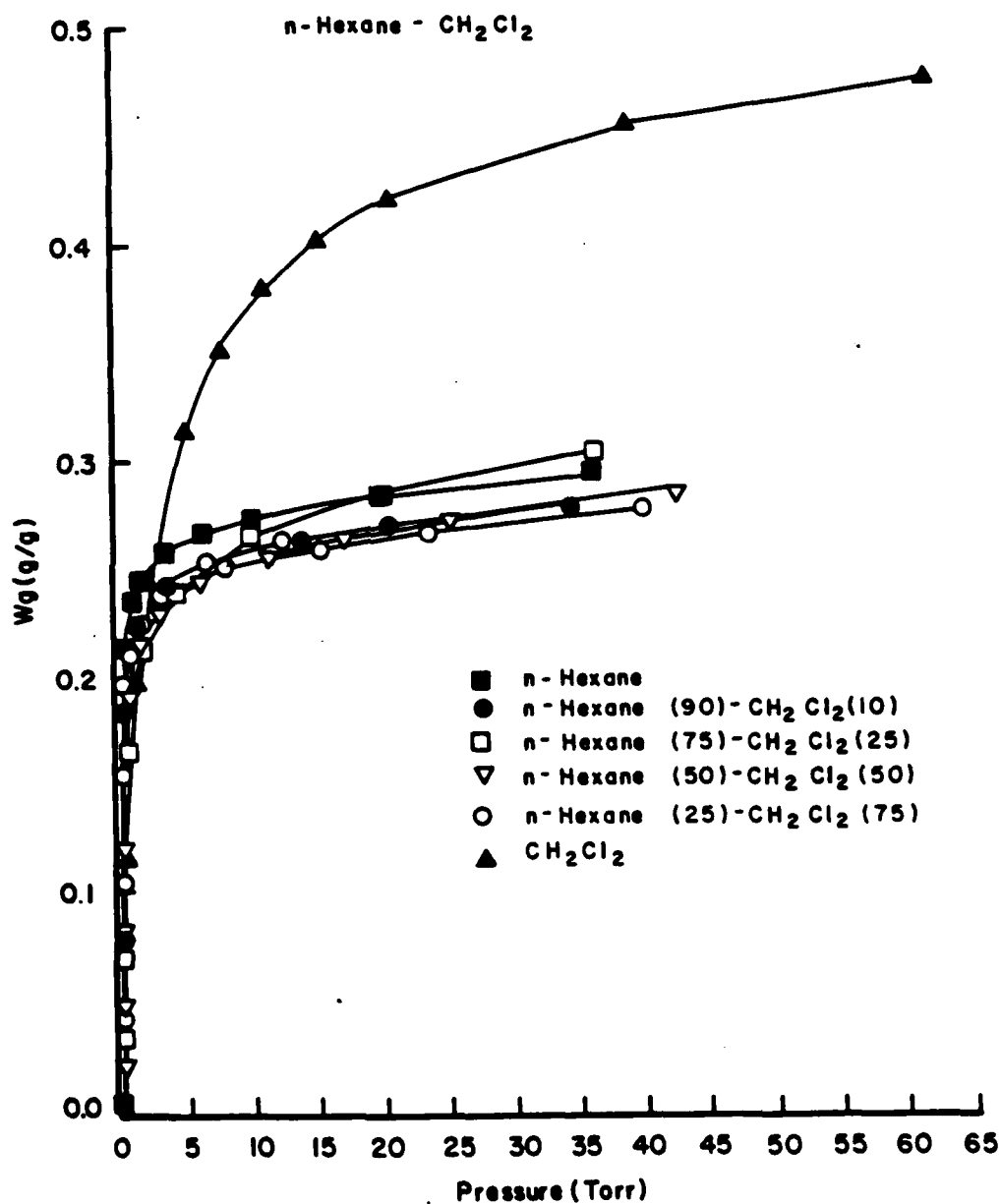


Figure 10. Single Vapor and Mixed Vapor Isotherms ($\text{C}_6\text{H}_{14} - \text{CH}_2\text{Cl}_2$ System) on BPL-Activated Carbon

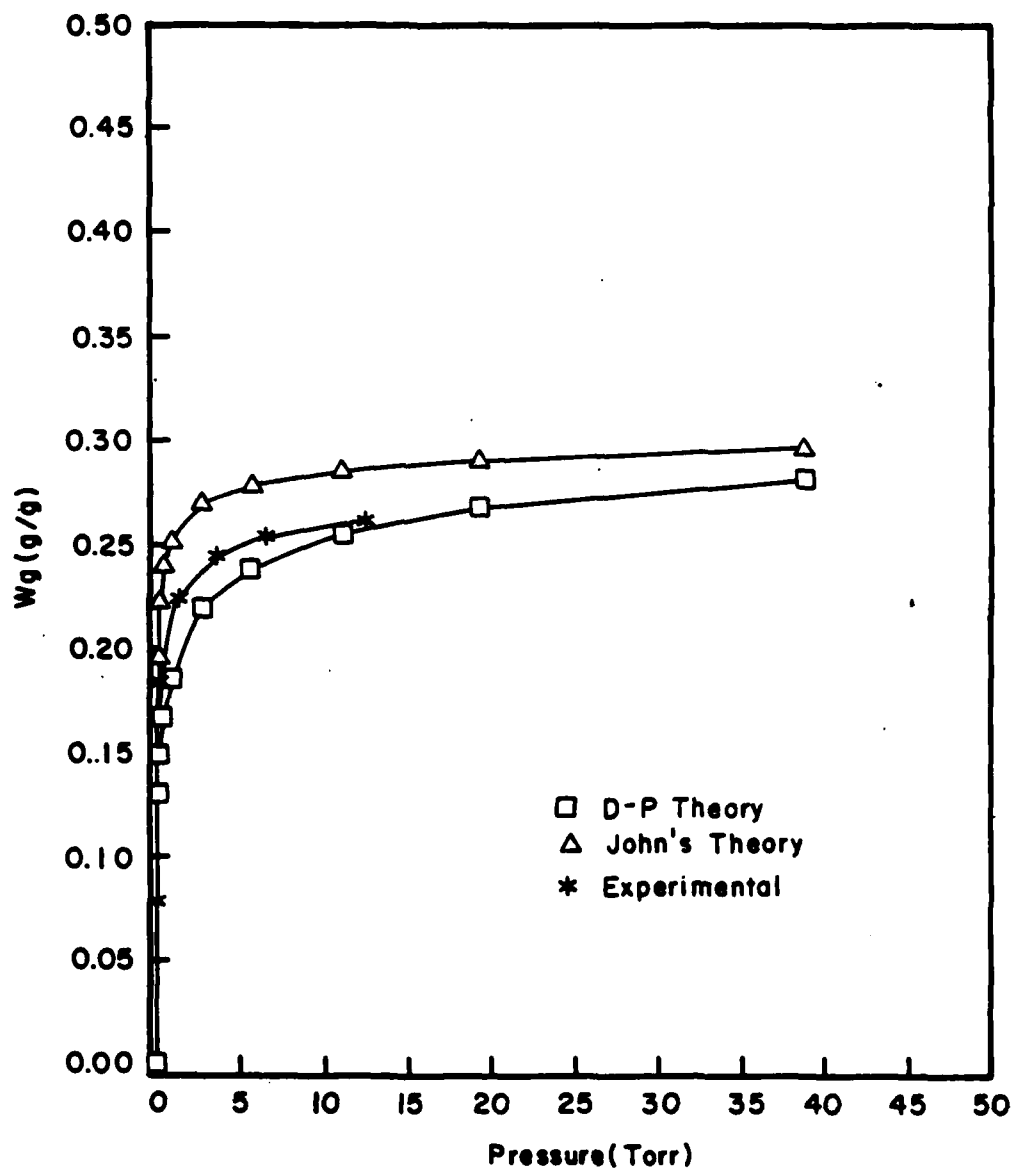


Figure 11. Experimental Mixed Vapor Isotherms ($C_6H_{14}(90)-CH_2Cl_2(10)$ Mixture) Compared with Theoretical Isotherms on BPL-Activated Carbon

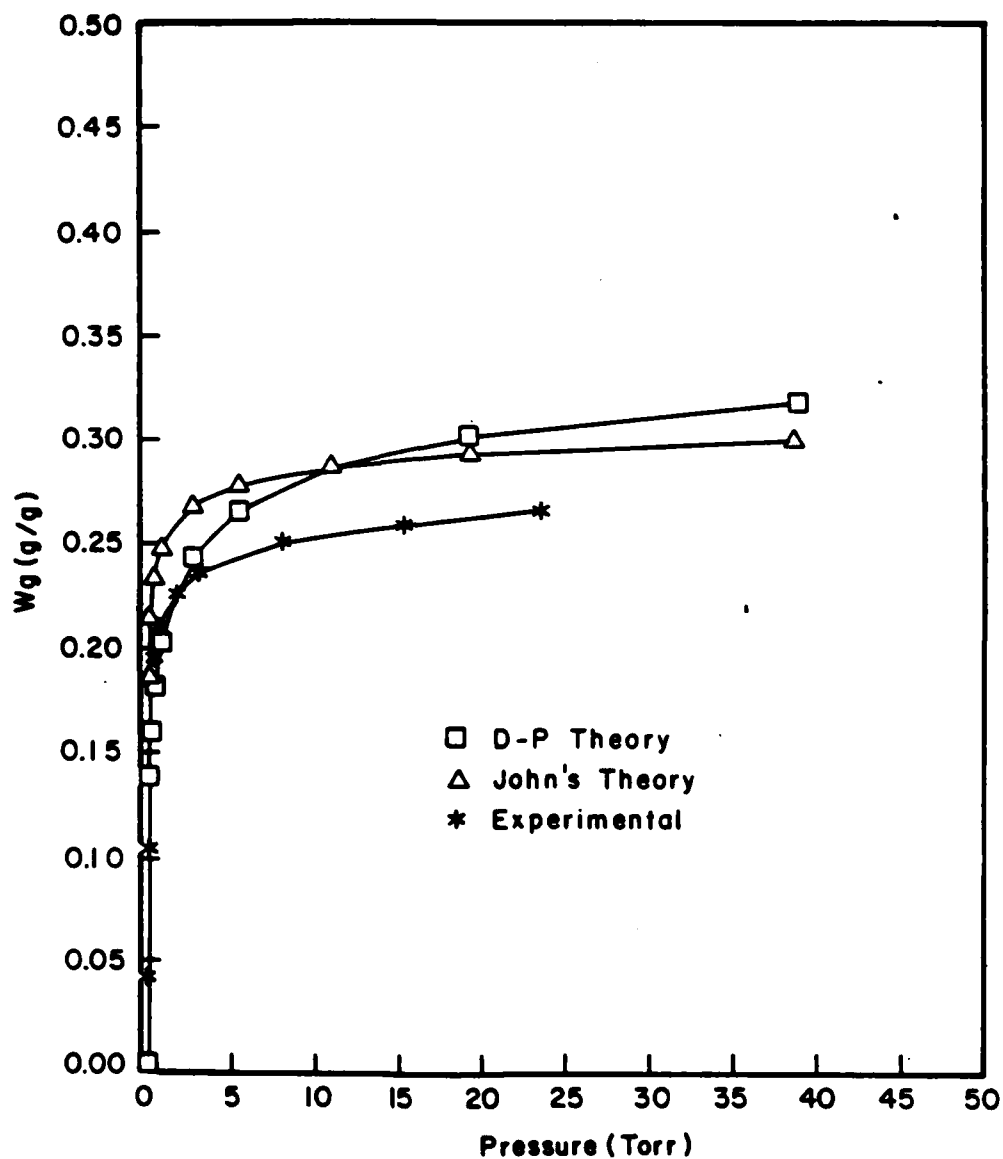


Figure 12. Experimental Mixed Vapor Isotherms ($C_6H_{14}(75)-CH_2Cl_2(25)$ Mixture) Compared with Theoretical Isotherms on BPL-Activated Carbon

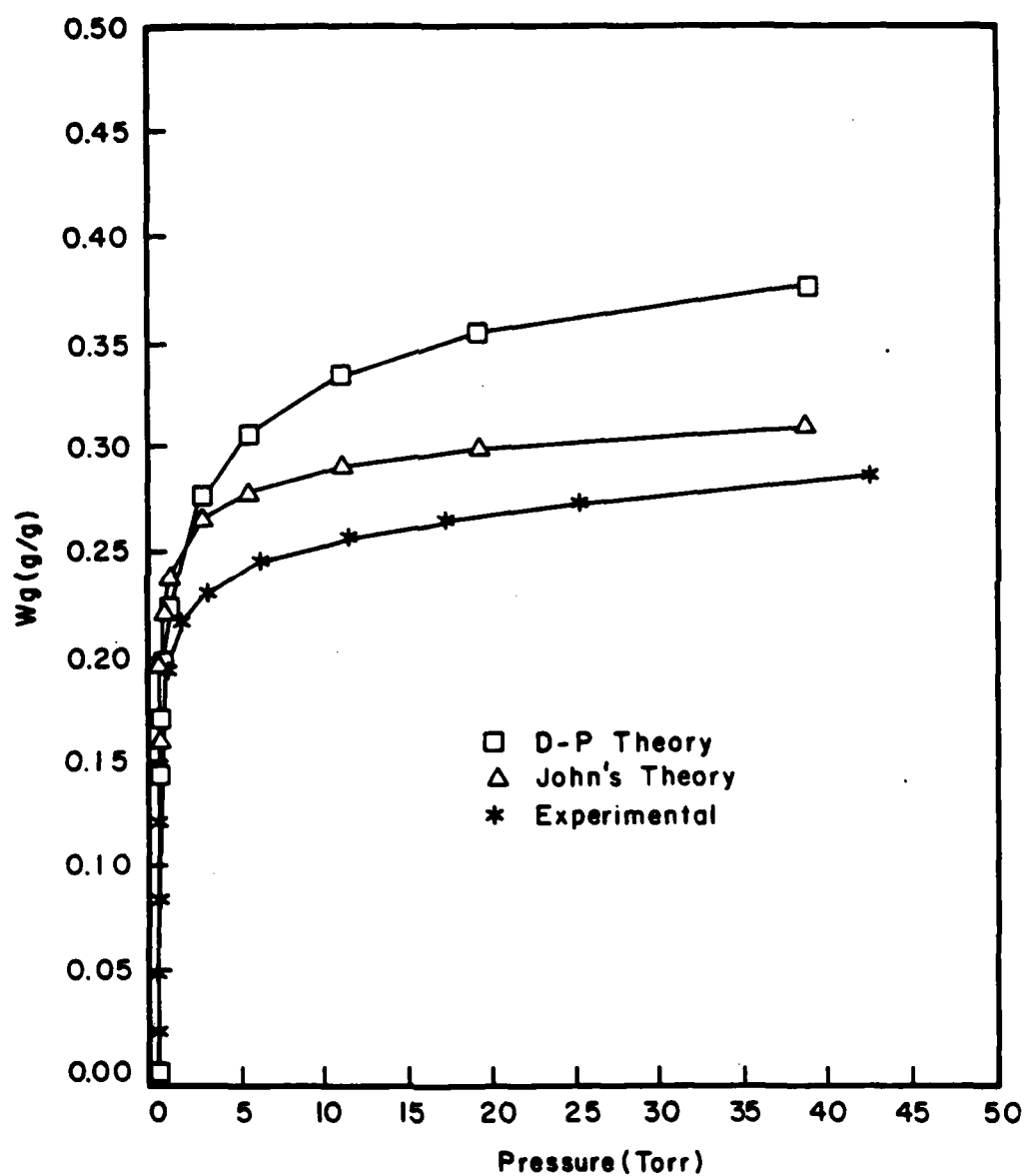


Figure 13. Experimental Mixed Vapor Isotherms ($C_6H_{14}(50)-CH_2Cl_2(50)$ Mixture) Compared with Theoretical Isotherms on BPL-Activated Carbon

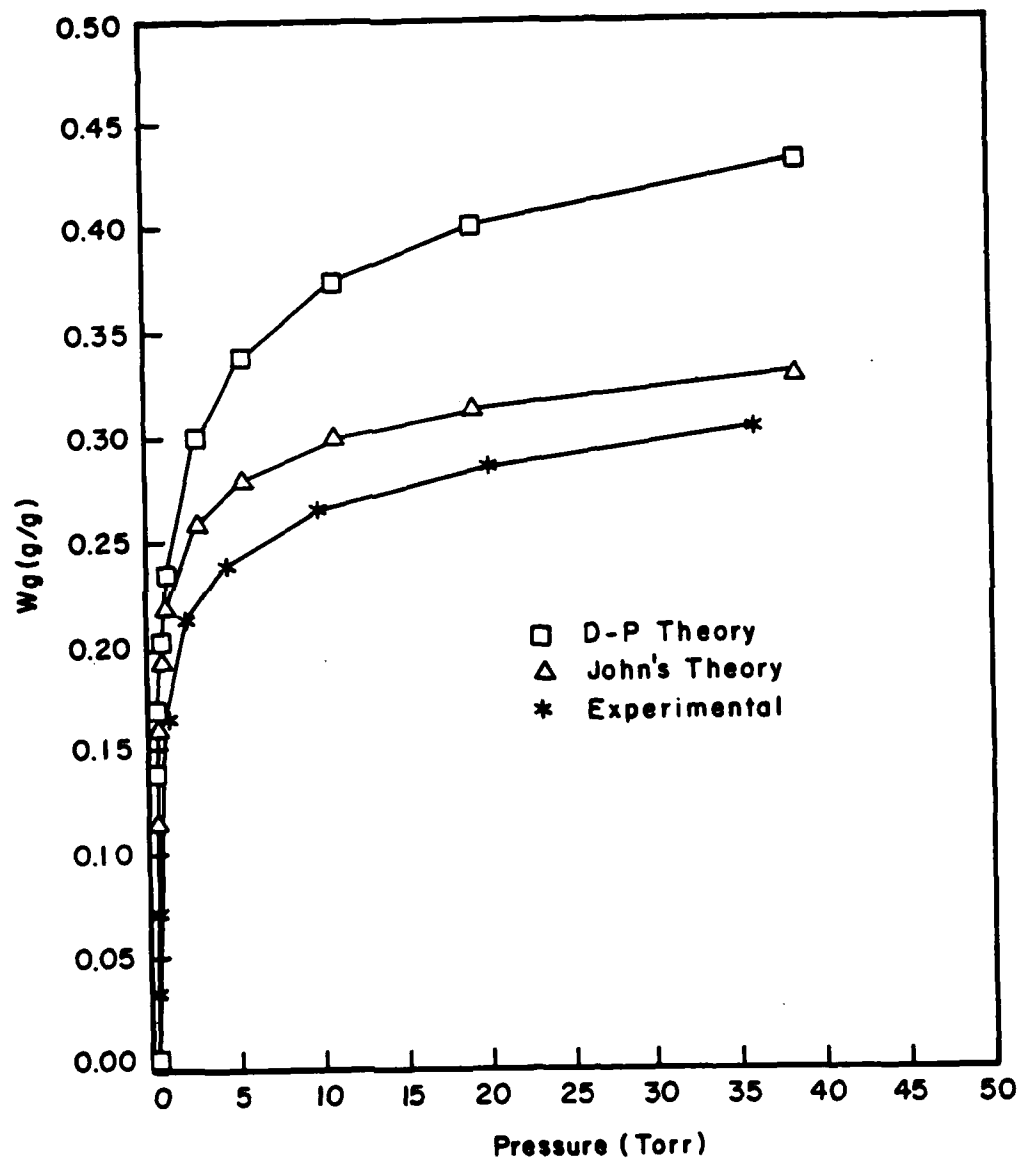


Figure 14. Experimental Mixed Vapor Isotherms $C_6H_{14}(25)-CH_2Cl_2(75)$ Mixture) Compared with Theoretical Isotherms on BPL-Activated Carbon

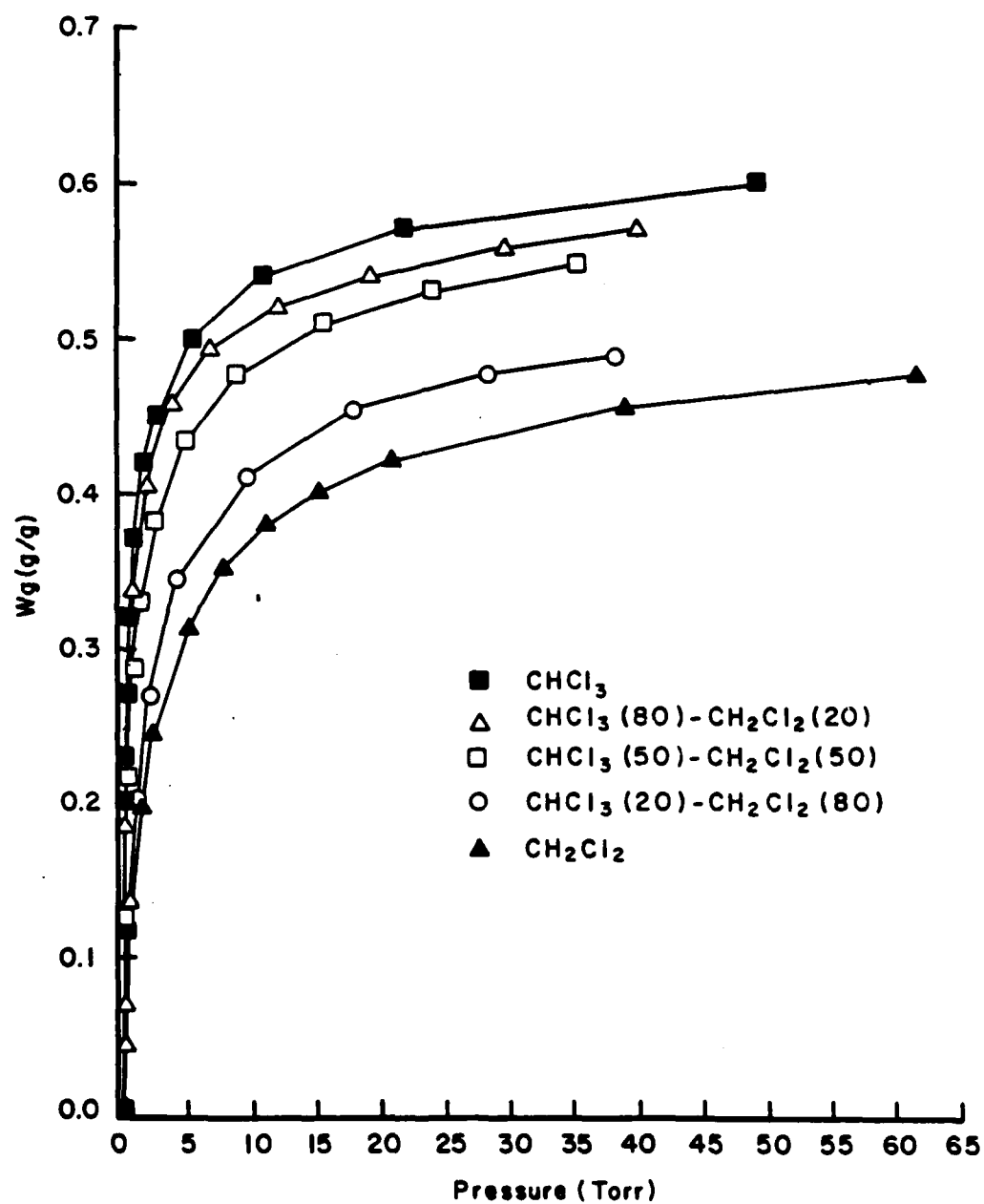


Figure 15. Single Vapor and Mixed Vapor Isotherms (CHCl_3 - CH_2Cl_2 System) on BPL-Activated Carbon

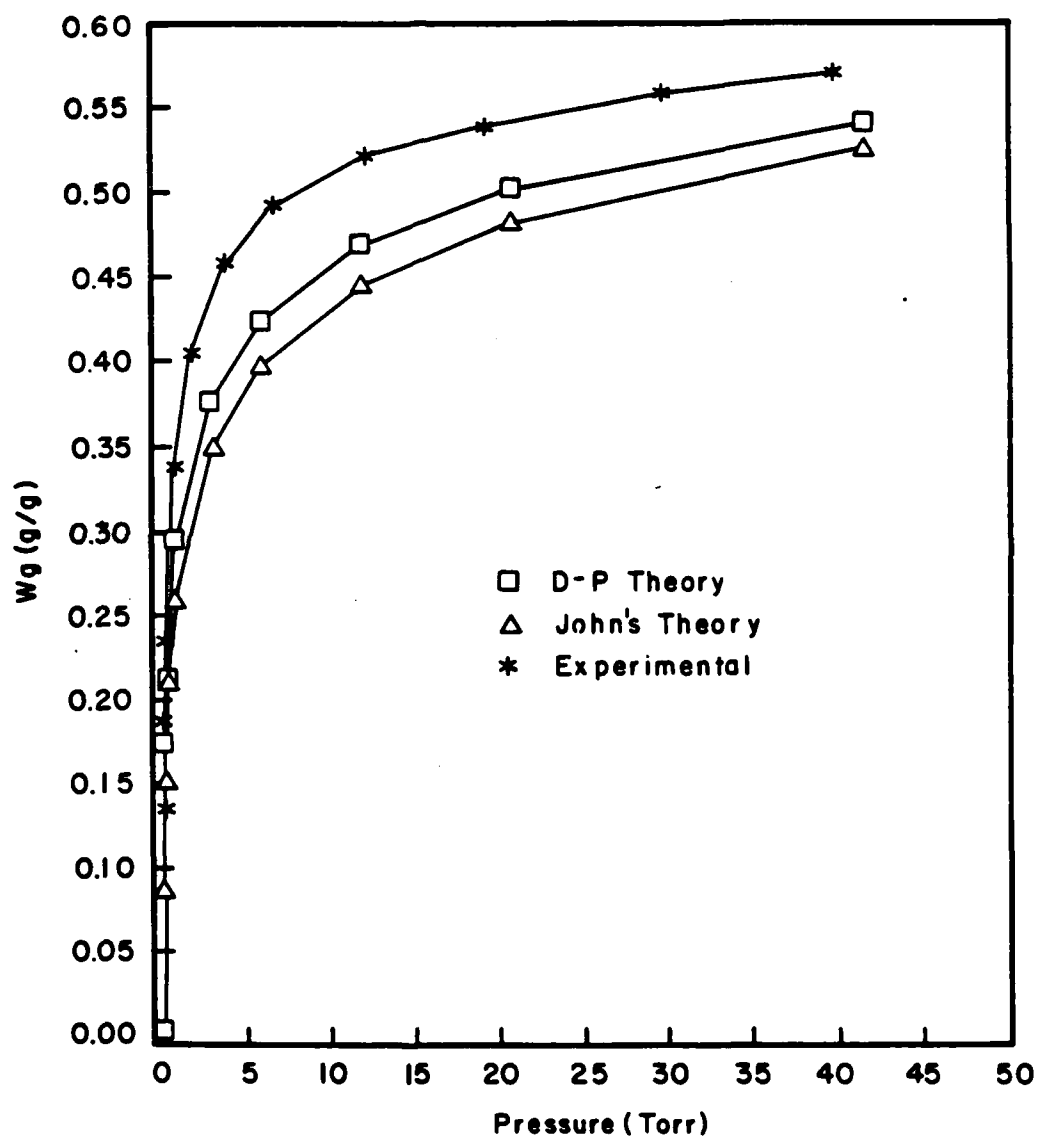


Figure 16. Experimental Mixed Vapor Isotherms ($\text{CHCl}_3(80)\text{-CH}_2\text{Cl}_2(20)$ Mixture) Compared with Theoretical Isotherms on BPL-Activated Carbon

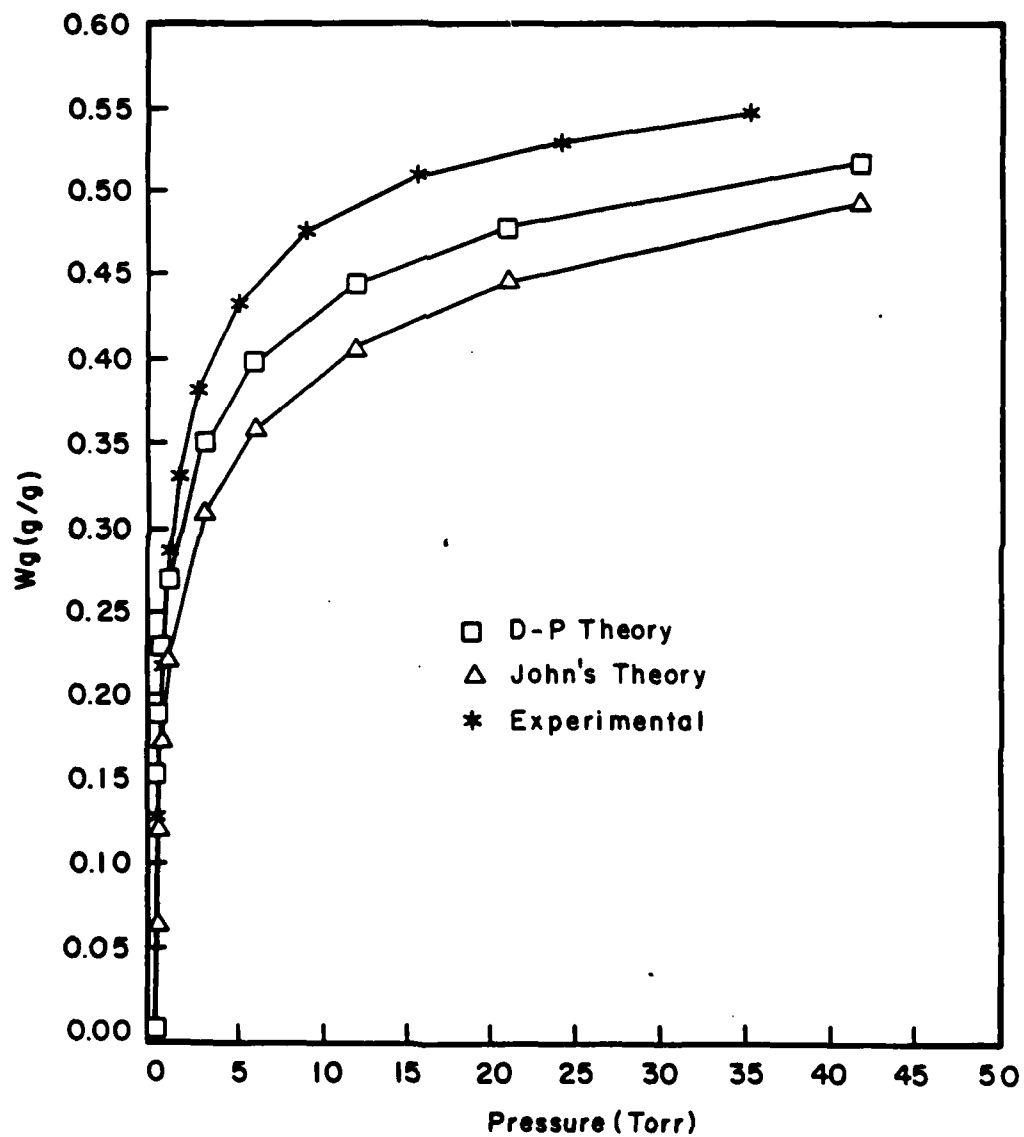


Figure 17. Experimental Mixed Vapor Isotherms ($\text{CHCl}_3(50)\text{-CH}_2\text{Cl}_2(50)$ Mixture) Compared with Theoretical Isotherms On BPL-Activated Carbon

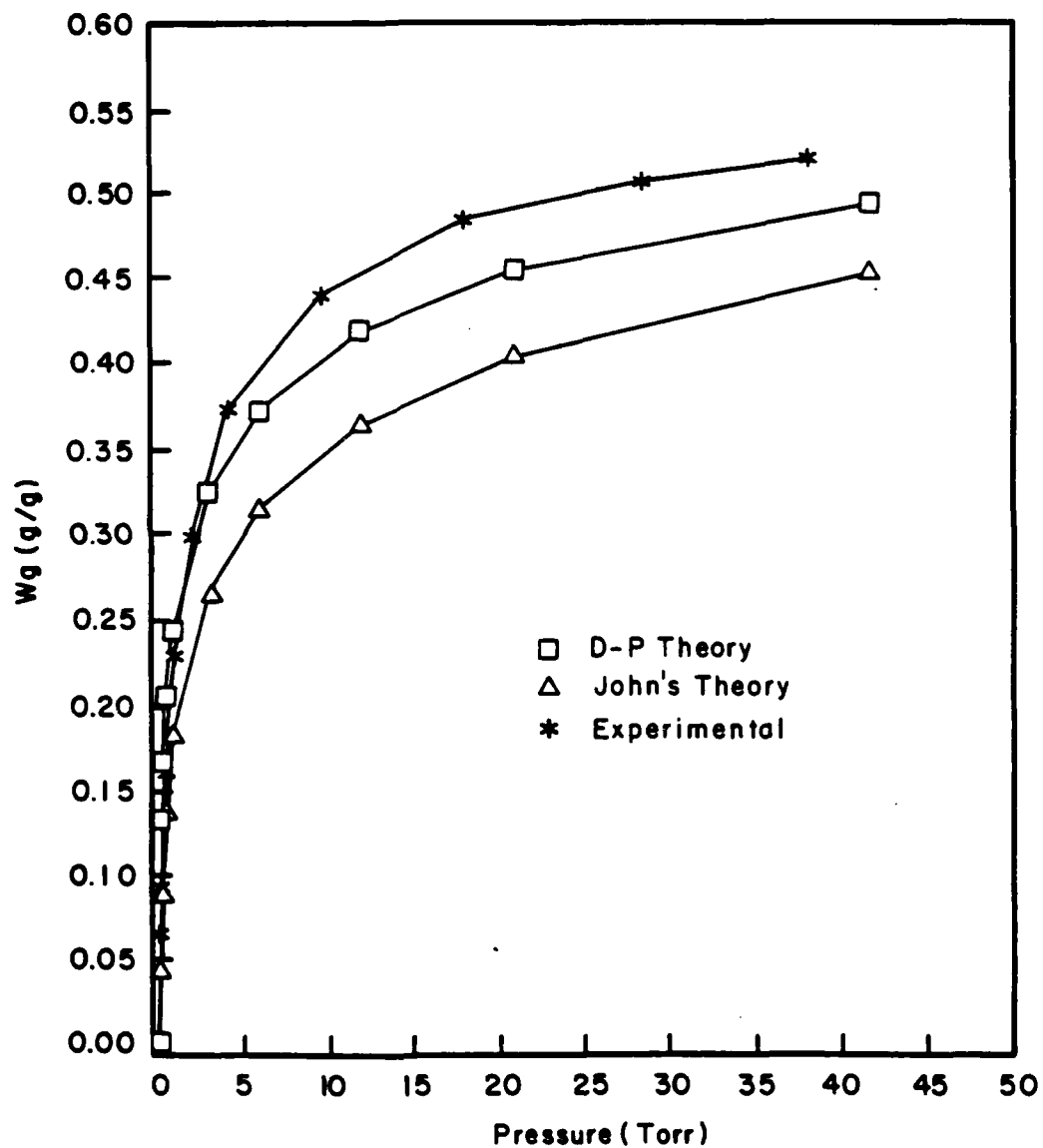


Figure 18. Experimental Mixed Vapor Isotherms ($\text{CHCl}_3(20)\text{-CH}_2\text{Cl}_2(80)$ Mixture) Compared with Theoretical Isotherms on BPL-Activated Carbon

also obtained by directly weighing the carbon bed before and after the adsorption process.

4.4 Results and Discussion.

A typical breakthrough curve for all the single vapors shows a sigmoidal shape. However, some of the components in the mixtures do not follow this behavior. All the investigated binary systems show that the component with a higher saturated vapor pressure is displaced regardless of the affinity coefficient. The displaced component does not generally follow a sigmoidal behavior. The displacement becomes evident when the C_x/C_o ratio is greater than 1.0. During this annual reporting period, additional kinetics studies were carried out for n-hexane/benzene (NP-NP) and for a new binary system CH_2Cl_2 /n-hexane (WP-NP). In addition, four theoretical models: DP theory, John's adsorption isotherm equation, the ideal adsorbed solution theory and the proportionality method were applied to all the binary mixtures in order to predict the adsorption capacities. Predicted values were then compared with kinetic and gravimetric capacities obtained experimentally.

Tables 1 and 2 show linear regression analysis of the t_b vs. W_b data for the two binary mixtures. The kinetic capacities, W_e , obtained from the regression analysis and listed in Tables 3 and 4 along with equilibrium capacities obtained gravimetrically (W_g) and the W_m values obtained by direct weighing.

In the case of the n-hexane/benzene mixture agreement between the three adsorption capacities (W_e , W_g and W_m) values is quite good. However, in the case of the CH_2Cl_2 /n-hexane (WP-NP) binary system, the kinetic experimental values, W_e , is considerably higher than both the capacity obtained by direct weighting (W_m) and the equilibrium gravimetric capacity (W_g). In the two binary systems ($CHCl_3/CCl_4$, $CH_2Cl_2/CHCl_3$)

studied last year, it was also observed that W_e values were always significantly higher than the W_g and W_m values. It is clear that Wheeler's

Table 1. Breakthrough Time (t_b) as a Function of Bed Weight (W_b) for the CH_2Cl_2 /n-Hexane Binary System on BPL-Activated Carbon. (Flow Rate = $400 \text{ cm}^3/\text{min.}$, $P_T = 25 \text{ torr}$, $T = 298^\circ\text{K}$).

| Mole Fraction CH_2Cl_2 | Bed Weight $W_b(\text{g})$ | Breakthrough Time t_b (min) | | Regression Equation | Correlation Coefficient |
|---|-------------------------------|-------------------------------|----------|----------------------------|-------------------------|
| | | CH_2Cl_2 | n-Hexane | | |
| 0.20 | 0.7000 | 2.98 | 2.99 | n-Hexane: | 1.000 |
| | 1.0007 | 4.00 | 4.37 | $t_b = 4.434 W_b - 0.101$ | |
| | 1.1999 | 5.00 | 5.20 | CH_2Cl_2 : | |
| | | | | $t_b = 3.989 W_b - 0.137$ | 0.994 |
| 0.50 | 0.7002 | 4.3 | 5.0 | n-Hexane: | 0.998 |
| | 0.8517 | 5.1 | 6.0 | $t_b = 7.317 W_b - 0.159$ | |
| | 1.0008 | 6.1 | 7.2 | CH_2Cl_2 : | |
| | | | | $t_b = 5.926 W_b - 0.073$ | 0.998 |
| 0.80 | 0.7003 | 4.0 | 9.4 | n-Hexane: | 1.000 |
| | 0.8505 | 4.98 | 11.8 | $t_b = 15.542 W_b - 1.475$ | |
| | 1.0007 | 6.5 | 14.0 | CH_2Cl_2 : | |
| | | | | $t_b = 8.29 W_b - 1.893$ | 0.997 |

equation is not quite effective when it is applied to weakly polar components in a mixture.

The mole fractions of the more volatile components in the adsorbed phase were calculated from the W_e values. These values, as a function of the mole fraction of the same component in the gas phase are shown in Figures 19 to 21 for the three mixtures n-hexane/benzene, $\text{CH}_2\text{Cl}_2/\text{CHCl}_3$ and n-hexane/ CH_2Cl_2 . It appears that the adsorbed phase mole fraction of CH_2Cl_2 in the CH_2Cl_2 /n-hexane binary system is similar in value to the mole fraction of CH_2Cl_2 in the gas phase, except at 70% or higher concentration. However, in the case of the n-hexane/benzene binary system, the mole fraction of n-hexane in the adsorbed phase is similar in value to the mole fraction of n-hexane in the gas phase only at low concentration (<0.3). In

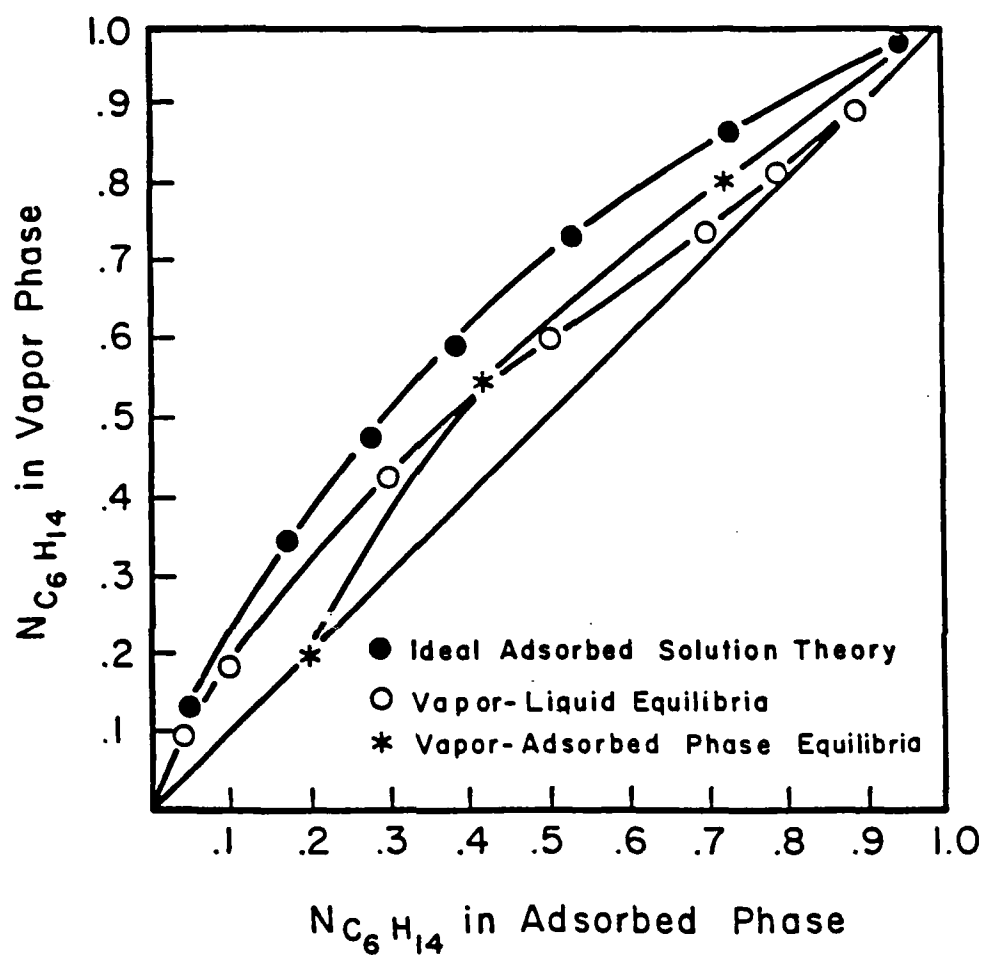


Figure 19. Vapor-Adsorbed Phase Equilibria for n-Hexane/Benzene Binary Mixture (BPL-Activated Carbon, $T = 25^\circ\text{C}$, $P_T = 25$ torr, flow rate = $400\text{ cm}^3/\text{min.}$)

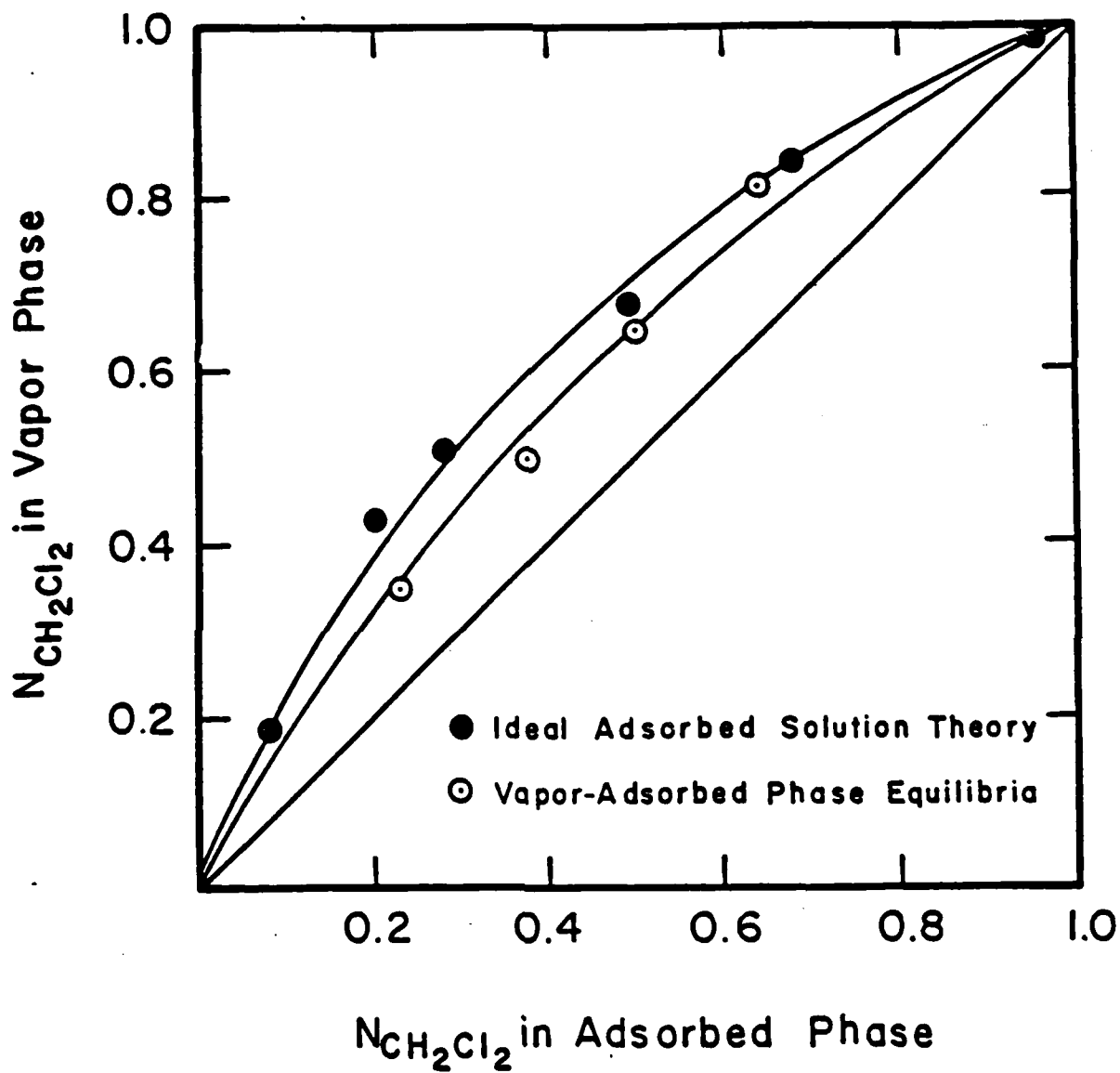


Figure 20. Vapor-Adsorbed Phase Equilibria for $\text{CHCl}_3/\text{CH}_2\text{Cl}_2$ Binary Mixture (BPL-Activated Carbon, $T = 25^\circ\text{C}$, $P_T = 25$ torr, flow rate = $400 \text{ cm}^3/\text{min.}$)

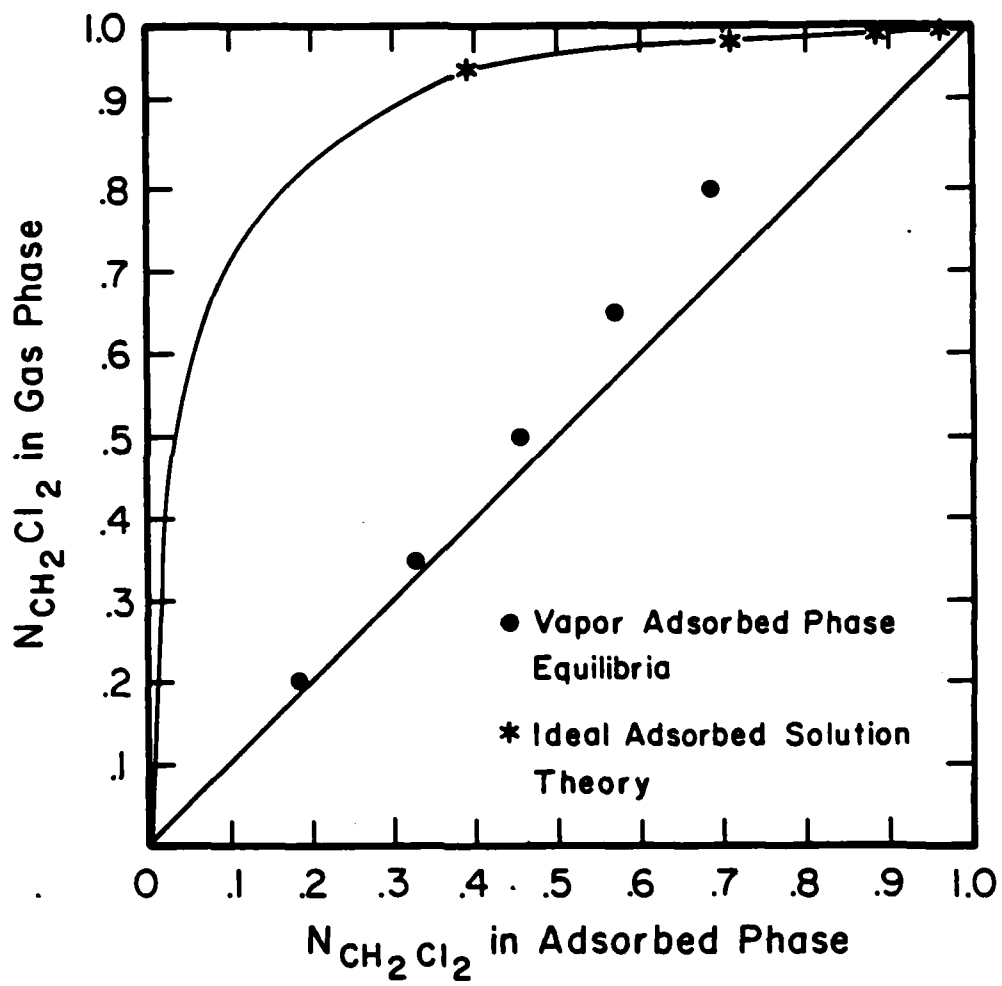


Figure 21. Vapor-Adsorbed Phase Equilibria for n-Hexane/ CH_2Cl_2 Binary Mixture (BPL-Activated Carbon, $T = 25^\circ\text{C}$, $P_T = 25$ torr, flow rate = $400 \text{ cm}^3/\text{min.}$)

Table 2. Breakthrough Time, t_b , as a Function of Composition and Bed Weight (W_b) for n-Hexane/Benzene Binary Mixtures*

| Mole Fraction ⁺ | t_b (min) | | W_b (g) | Regression |
|----------------------------|-------------|--------|-----------|--|
| | n-Hexane | Benzen | | |
| 0.0 | - | 5.15 | 0.8000 | Benzene: $t_b = 7.7743W_b - 1.0403$ corr. = 0.9999 |
| | - | 6.00 | 0.9037 | |
| | - | 7.55 | 1.1006 | |
| | - | 9.85 | 1.4033 | |
| 0.2 | 4.50 | 4.50 | 0.8004 | Benzene: $t_b = 7.4478W_b - .0839$ corr. = .998 n-Hexane: $t_b = 7.1996W_b - 1.2630$ corr. = 1.0000 |
| | 5.95 | 5.95 | 1.0020 | |
| | 7.40 | 7.50 | 1.2032 | |
| 0.35 | 3.80 | 4.20 | 0.7002 | Benzene: $t_b = 6.27W_b - 0.3589$ corr. = 0.997 n-Hexane: $t_b = 5.37W_b - 0.0610$ corr. = 0.9996 |
| | 4.60 | 4.85 | 0.8509 | |
| | 5.50 | 5.80 | 1.0003 | |
| | 7.55 | 8.50 | 1.4000 | |
| 0.50 | 3.75 | 4.10 | 0.7005 | Benzene: $t_b = 6.1813W_b - 0.6835$ corr. = 0.998 n-Hexane: $t_b = 6.2459W_b - 0.5003$ |
| | 4.45 | 4.50 | 0.8515 | |
| | 5.55 | 5.85 | 1.0018 | |
| | 6.65 | 6.90 | 1.2001 | |
| | 8.10 | 8.40 | 1.4097 | |
| 0.80 | 3.70 | 3.20 | 0.7019 | Benzene: $t_b = 10.1161W_b - 4.1374$ corr. = 0.9961 n-Hexane: $t_b = 5.6232W_b - 0.2830$ corr. = 0.9997 |
| | 4.45 | 4.15 | 0.8502 | |
| | 7.10 | 9.20 | 1.3109 | |
| 1.00 | 4.2 | - | 0.5997 | n-Hexane: $t_b = 8.1474W_b - 1.049$ corr. = 0.9998 |
| | 4.5 | - | 0.6875 | |
| | 5.9 | - | 0.8498 | |
| | 7.1 | - | 0.9934 | |
| | 10.35 | - | 1.4028 | |

*BPL-Activated Carbon, Flow Rate = 400 cm³/min, 25°C, and P_{total} = 25 torr.

⁺Vapor Phase

Table 3. Kinetic Saturation Capacities (W_e), Direct Weight Saturation Capacities (W_m) and Equilibrium Capacities (W_g) for the CH_2Cl_2 /n-Hexane Binary System on BPL-Activated Carbon. (Flow rate = $400 \text{ cm}^3/\text{min.}$, $P_T = 25 \text{ torr}$, $T = 298^\circ\text{K}$)

| Mole Fraction | W_e | | W_e | W_g | W_m |
|---------------|--------------------------|---------------------------|--------|--------|-------|
| | CH_2Cl_2 | C_6H_{14} | Total | g/g | g/g |
| 0.2 | 0.0364 | 0.1645 | 0.2009 | 0.270 | 0.298 |
| 0.5 | 0.1370 | 0.1690 | 0.3060 | 0.2725 | 0.252 |
| 0.8 | 0.3030 | 0.1442 | 0.4472 | 0.290 | 0.266 |

Table 4. Kinetic Saturation Capacities (W_e), Direct Weight Saturation Capacities (W_m) and Equilibrium Capacities (W_g) for the C_6H_6 /n-Hexane Binary System on BPL-Activated Carbon (Flow rate = $400 \text{ cm}^3/\text{min.}$, $P_T = 25 \text{ torr}$, $T = 298^\circ\text{K}$)

| Mole Fraction | W_e | | W_e | W_g | W_m |
|---------------|----------|---------------------------|-------|-------|-------|
| | n-hexane | C_6H_{14} | Total | g/g | g/g |
| | | C_6H_6 | | | |
| 0.0 | --- | 0.330 | 0.330 | 0.370 | 0.328 |
| 0.2 | 0.067 | 0.250 | 0.318 | 0.318 | 0.335 |
| 0.5 | 0.130 | 0.144 | 0.275 | 0.312 | 0.312 |
| 0.8 | 0.208 | 0.085 | 0.296 | 0.302 | 0.285 |
| 1.0 | 0.226 | --- | 0.226 | 0.270 | 0.252 |

the case of the $\text{CH}_2\text{Cl}_2/\text{CHCl}_3$ binary system ($N_{\text{CH}_2\text{Cl}_2} = 0.35, 0.5 \text{ and } 0.65$ data were reported in the last year's report) the mole fraction of CH_2Cl_2 in the adsorbed phase is less than the gas phase value for the whole range of concentration studied. It appears that each system behaves differently.

As mentioned previously, all four theories have been applied to the $\text{CHCl}_3/\text{CCl}_4$, n-hexane/benzene, $\text{CH}_2\text{Cl}_2/\text{CHCl}_3$ and n-hexane/ CH_2Cl_2 binary mixtures in order to predict the adsorption capacities. The results are shown in Tables 5-8 for all four models investigated. These tables also compare the kinetic adsorption capacities calculated from Wheeler's equation. The maximum deviation of the predicted capacities, with respect to W_g , for all Binary mixtures except n-hexane/ CH_2Cl_2 , ranges from -7.0% to 19%. In the case of n-hexane/ CH_2Cl_2 , the comparison indicates that none of the models are particularly successful in predicting the correct amount adsorbed (the deviation ranges from 19% to 91%). Also it is not possible to employ the ideal adsorbed solution theory for this particular binary at the given experimental conditions. It appears that a large saturated vapor

Table 5. Comparison of Adsorption Capacities Obtained from Several Predictive Models with the Experimental Values (W_e & W_g) for the Benzene/n-Hexane Mixture ($P_T = 25$ torr, flow rate = $400 \text{ cm}^3/\text{min}$)

| Mole Fraction | Predicted Sorption g/g | | | | | | | | W _e | W _g |
|---------------|------------------------|--------|------------------|--------|------------------|--------|-------------------------|--------|----------------|----------------|
| | DP-Model | | John's Model | | Myers' Model | | Proportionality Method* | | | |
| n-Hexane | W _{mix} | % Dev+ | W _{mix} | % Dev+ | W _{mix} | % Dev+ | W _{mix} | % Dev+ | g/g | g/g |
| 0.0 | | | | | | | | | 0.330 | 0.370 |
| 0.20 | 0.340 | -7.0% | 0.326 | -2.5% | 0.337 | -5.3% | 0.319 | 0.3% | 0.318 | 0.318 |
| 0.50 | 0.318 | -1.9% | 0.314 | -0.6% | 0.323 | -3.5% | 0.307 | 1.6% | 0.275 | 0.312 |
| 0.80 | 0.295 | 2.3% | 0.300 | -0.6% | 0.312 | 3.3% | 0.296 | 2.0% | 0.295 | 0.302 |
| 1.00 | | | | | | | | | 0.226 | 0.270 |

$$*W_{\text{mix}} = (N_{\text{Benzene}} \times W_{\text{Benzene}}) + (N_{\text{n-Hexane}} \times W_{\text{n-Hexane}})$$

+With respect to W_g

Table 6. Comparison of Adsorption Capacities Obtained from Several Predictive Models with the Experimental Values (W_e & W_g) for the $\text{CHCl}_3/\text{CCl}_4$ Mixture ($P_T = 25$ torr, flow rate = $400 \text{ cm}^3/\text{min}$)

| Mole Fraction | Predicted Sorption g/g | | | | | | | | W _e | W _g |
|-------------------|------------------------|--------|------------------|--------|------------------|--------|-------------------------|--------|----------------|----------------|
| | DP-Model | | John's Model | | Myers' Model | | Proportionality Method* | | | |
| CHCl ₃ | W _{mix} | % Dev+ | W _{mix} | % Dev+ | W _{mix} | % Dev+ | W _{mix} | % Dev+ | g/g | g/g |
| 0.0 | | | | | | | | | 0.696 | 0.669 |
| 0.20 | 0.636 | 1.9% | 0.609 | -2.4% | 0.658 | 5.4% | 0.616 | -1.2% | 0.786 | 0.624 |
| 0.50 | 0.621 | 2.1% | 0.590 | -3.0% | 0.636 | 4.6% | 0.599 | -1.5% | 0.796 | 0.608 |
| 0.80 | 0.607 | 4.3% | 0.569 | -2.2% | 0.605 | 4.0% | 0.582 | 0 | 0.722 | 0.582 |
| 1.00 | | | | | | | | | 0.781 | 0.585 |

$$*W_{\text{mix}} = (N_{\text{CHCl}_3} \times W_{\text{CHCl}_3}) + (N_{\text{CCl}_4} \times W_{\text{CCl}_4})$$

+With respect to W_g

pressure (P_0) difference and large difference in affinity coefficient (β) between the two components plays an important role in determining the binary vapor adsorption characteristics. Table 9 lists the difference in affinity coefficient and saturated vapor pressure for the binary systems.

In addition to the total amount of a mixture adsorbed (W_{12}), it is also important to be able to predict the amount of each binary component that contributes to W_{12} . A semi-empirical formula suggested by Lewis²⁰ can be used, in principle, to predict the amount of each binary component adsorbed:

$$W_1/W_2^0 + W_2/W_2^0 = 1$$

where $W_1 + W_2 = W_{12}$ and W_1 , W_2 , W_{12} are the amounts adsorbed of component 1, component 2 and the mixture at pressures:

$$P_{12} = P_1^0 = P_2^0 \quad (\text{note } P_{12} = P_1 + P_2).$$

There is also the proportionality method as mentioned previously that can be used to predict the amount of each binary component adsorbed:

$$W_{12} = W_1 N_1 + W_2 N_2$$

These two methods were applied to calculate the adsorption capacities of individual components at a total pressure of 25 torr and at different compositions for the $\text{CH}_2\text{Cl}_2/\text{CHCl}_3$, n-hexane/ CH_2Cl_2 and the n-hexane/benzene binary systems. Comparison of the predicted and the experimental adsorption capacities are shown in Tables 10-12.

Table 7. Comparison of Adsorption Capacities Obtained from Several Predictive Models with that of Experimental Capacities (W_e and W_g) for the $\text{CHCl}_3/\text{CH}_2\text{Cl}_2$ Mixture ($P_T = 25$ torr, flow rate = $400 \text{ cm}^3/\text{min}$)

| Mole Fraction | Predicted Sorption, g/g | | | | | | | | W_e g/g | W_g g/g |
|--------------------------|-------------------------|-------------------|------------------|-------------------|------------------|-------------------|-------------------------|-------------------|--------------|--------------|
| | DP-Model | | John's Model | | Myers' Model | | Proportionality Method* | | | |
| | W_{mix} | %Dev ⁺ | W_{mix} | %Dev ⁺ | W_{mix} | %Dev ⁺ | W_{mix} | %Dev ⁺ | | |
| CH_2Cl_2 | | | | | | | | | | |
| 0.0 | -- | -- | -- | -- | -- | -- | -- | -- | 0.692 | 0.585 |
| 0.20 | 0.549 | 0.9% | 0.568 | -2.5% | 0.541 | 2.4% | 0.562 | -1.4% | 0.933 | 0.554 |
| 0.50 | 0.486 | 8.8% | 0.521 | 2.3% | 0.498 | 6.6% | 0.515 | 3.4% | 0.950 | 0.533 |
| 0.80 | 0.405 | 19.4% | 0.471 | 6.4% | 0.453 | 9.9% | 0.467 | 7.2% | 0.722 | 0.503 |
| 1.00 | -- | -- | -- | -- | -- | -- | -- | -- | 0.478 | 0.323 |

$$* W_{\text{mix}} = \left(N_{\text{CH}_2\text{Cl}_2} \times W_{\text{CH}_2\text{Cl}_2} \right) + \left(N_{\text{CHCl}_3} \times W_{\text{CHCl}_3} \right)$$

⁺ % deviation with respect to W_g

Table 8. Comparison of Adsorption Capacities Obtained from Several Predictive Models with the Experimental Values (W_e and W_g) for the CH_2Cl_2 /n-Hexane Mixture ($P_T = 25$ torr, flow rate = $400 \text{ cm}^3/\text{min}$)

| Predicted Sorption, g/g | | | | | | | | | | |
|--------------------------|------------------|-------------------|------------------|-------------------|------------------|-------------------|-------------------------|-------------------|-------|-------|
| Mole Fraction | DP-Model | | John's Model | | Myers' Model | | Proportionality Method* | | W_e | W_g |
| CH_2Cl_2 | W_{mix} | %Dev ⁺ | W_{mix} | %Dev ⁺ | W_{mix} | %Dev ⁺ | W_{mix} | %Dev ⁺ | g/g | g/g |
| | | | | | | | | | | |
| 0.2 | 0.330 | 22.9 | 0.512 | 90.0 | -- | -- | 0.319 | 19.1 | 0.201 | 0.270 |
| 0.5 | 0.372 | 27.8 | 0.507 | 74.2 | -- | -- | 0.354 | 21.5 | 0.306 | 0.273 |
| 0.8 | 0.385 | 32.8 | 0.497 | 71.3 | -- | -- | 0.388 | 33.7 | 0.447 | 0.290 |

$$* W_{\text{mix}} = (N_{\text{CH}_2\text{Cl}_2} \times W_{\text{CH}_2\text{Cl}_2}) + (N_{\text{n-Hexane}} \times W_{\text{n-Hexane}})$$

⁺ With respect to W_g .

Table 9. Affinity Coefficient Difference and Saturated Vapor Pressure Difference of Components in Mixtures Investigated

| Mixture | Affinity Coeff Difference | Saturate Vapor Press Diff. |
|--|---------------------------|----------------------------|
| $\text{CCl}_4\text{-CHCl}_3$ (NP-WP) | 0.11 | 83 torr |
| $\text{CHCl}_3\text{-CH}_2\text{Cl}_2$ (WP-WP) | 0.39 | 205 |
| $\text{C}_6\text{H}_6\text{-C}_6\text{H}_{14}$ (NP-NP) | 0.28 | 54.6 |
| $\text{C}_6\text{H}_{14}\text{-CH}_2\text{Cl}_2$ (NP-WP) | 0.70 | 249.5 |
| $\text{C}_6\text{H}_{14}\text{-CH}_3\text{COCH}_3$ (NP-SP) | 0.61 | 175 |

Table 10 shows that the maximum percentage deviations of the capacity

Table 10. Calculated Capacities (Methods 1 and 2) and Experimental Kinetic Capacities (W_e) for the n-Hexane/Benzene Mixture on BPL-Activated Carbon ($P_T = 25$ torr and flow rate of $400 \text{ cm}^3/\text{min}$)

| Mole Fraction | Calculated & Kinetic Capacities (g/g) | | | Calculated & Kinetic Capacities (g/g) | | | Dev % | | | |
|---------------|---------------------------------------|------------|---------------|---------------------------------------|------------|---------------|-----------|-----------|-----------|-----------|
| | n-Hexane | | | Benzene | | | n-Hexane | Benzene | | |
| n-Hexane | Method #1* | Method #2† | Kinetic W_e | Method #1* | Method #2† | Kinetic W_e | Method #1 | Method #2 | Method #1 | Method #2 |
| | | | | | | | | | | |
| 0.0 | - | - | - | 0.330 | 0.330 | 0.330 | - | - | 0 | 0 |
| 0.2 | 0.0710 | 0.0473 | 0.067 | 0.248 | 0.275 | 0.250 | 5.96 | -30.0 | -0.01 | 0.1 |
| 0.5 | 0.142 | 0.153 | 0.130 | 0.162 | 0.153 | 0.144 | 9.2 | 17.6 | 12.5 | 6.25 |
| 0.8 | 0.213 | 0.247 | 0.204 | 0.083 | 0.0431 | 0.089 | 4.41 | 21.1 | -6.74 | -51.5 |
| 1.0 | 0.283 | 0.283 | 0.225 | - | - | - | 25.8 | 25.8 | - | - |

* Assuming $W_{\text{Mixture}} = N_{\text{n-hexane}} W_{\text{n-hexane}} + N_{\text{benzene}} W_{\text{benzene}}$

† From Lewis's Equation

Table 11. Calculated Capacities (Methods 1 and 2) and Experimental Kinetic Capacities (W_e) for the $\text{CH}_2\text{Cl}_2/\text{CHCl}_3$ Mixture on BPL-Activated Carbon ($P_T = 25$ torr and flow rate of 400 cm^3/min)

| Mole Fraction | Calculated & Kinetic Capacities (g/g) CHCl_3 | | Calculated & Kinetic Capacities (g/g) CH_2Cl_2 | | Dev % CHCl_3 | | Dev % CH_2Cl_2 | |
|--------------------------|--|------------|---|------------|-----------------------|-----------|--------------------------------|-----------|
| | Method #1* | Method #2† | Method #1* | Method #2† | Method #1 | Method #2 | Method #1 | Method #2 |
| CH_2Cl_2 | | | | | | | | |
| 0.0 | 0.574 | 0.574 | 0.692 | - | -17.0 | -17.0 | - | - |
| 0.2 | 0.459 | 0.528 | 0.761 | 0.0857 | -39.6 | -30.6 | -50.0 | -80.0 |
| 0.5 | 0.288 | 0.510 | 0.693 | 0.215 | -58.4 | -26.4 | 16.3 | -81.1 |
| 0.8 | 0.114 | 0.435 | 0.422 | 0.342 | -73.0 | 3.8 | 14.0 | -65.3 |
| 1.00 | - | - | - | 0.428 | - | - | -10.4 | -10.4 |

* Assuming $W_{\text{Mixture}} = N_{\text{CHCl}_3} W_{\text{CHCl}_3} + N_{\text{CH}_2\text{Cl}_2} W_{\text{CH}_2\text{Cl}_2}$

† From Lewi's Equation

Table 12. Calculated Capacities (Methods 1 and 2) and Experimental Kinetic Capacities (W_e) for the n-Hexane/ CH_2Cl_2 Mixture on BPL-Activated Carbon ($P_T = 25$ torr and flow rate of 400 cm^3/min)

| Mole Fraction | Calculated & Kinetic Capacities (g/g) n-Hexane | | Calculated & Kinetic Capacities (g/g) CH ₂ Cl ₂ | | Dev % n-Hexane | Dev % CH ₂ Cl ₂ |
|---------------------------------|--|------------|---|-----------------------|-----------------------|---------------------------------------|
| | Method #1* | Method #2+ | Kinetic W _e | Method #1* Method #2+ | | |
| CH ₂ Cl ₂ | Method #1* | Method #2+ | Kinetic W _e | Method #1* Method #2+ | Method #1* Method #2+ | Method #1* Method #2+ |
| 0.0 | 0.283 | 0.283 | 0.225 | - 25.8 | 25.8 | |
| 0.2 | 0.213 | 0.247 | 0.204 | 0.0857 0.034 | 4.4 21.1 | -50.0 -80.0 |
| 0.5 | 0.142 | 0.153 | 0.130 | 0.215 0.048 | 9.20 17.69 | 16.3 -81.1 |
| 0.8 | 0.0710 | 0.0473 | 0.067 | 0.342 0.104 | 5.97 -29.4 | 14.0 -65.3 |
| 1.00 | - | - | - | 0.428 0.428 | - - | -10.4 -10.4 |

* Assuming $W_{\text{Mixture}} = N_{\text{n-Hexane}} + N_{\text{CH}_2\text{Cl}_2} + W_{\text{CH}_2\text{Cl}_2}$

+From Lewis's Equation

using Methods 1 and 2 for n-hexane are 26% and 30% respectively. However, the capacities calculated for benzene in this mixture using the same models gave small percentage deviation. In the case of the $\text{CH}_2\text{Cl}_2/\text{CHCl}_3$ binary system, both the methods showed very poor agreement with the experimental data. For the CH_2Cl_2 /n-hexane mixture, none of the methods were successful in predicting the amount adsorbed of each individual component. Deviations range from 4% to 80%. The dichloromethane/n-hexane mixture has the largest difference in properties compared to the other systems. Preliminary studies on the acetone/n-hexane mixture also indicate similar behavior. For these particular types of mixtures, the mixture with a higher affinity coefficient (n-hexane) seems to dominate the adsorption behavior.

From the studies on these four mixtures, it has become apparent that each mixture behaves differently. NP-NP mixtures are ideal for studies. Most of the theoretical models are successful in predicting the adsorption isotherms for NP-NP mixtures. However, deviation from theory becomes greater as:

- 1) Polarity is introduced into the mixture.
- 2) Difference in affinity coefficient of the two components is large.
- 3) There is a large difference in saturated vapor pressure.

5. RECOMMENDATIONS FOR FUTURE WORK

Efforts within the last two years have dealt with detailed kinetic and equilibrium adsorption studies of $\text{CHCl}_3/\text{CCl}_4$ (WP-NP), $\text{CHCl}_3/\text{CH}_2\text{Cl}_2$ (WP-WP), $\text{C}_6\text{H}_{14}/\text{C}_6\text{H}_6$ (NP-NP) and $\text{CH}_2\text{Cl}_2/\text{C}_6\text{H}_{14}$ (WP-NP) binary mixtures and single vapors on BPL-activated carbon. In addition, preliminary results have been obtained in the case of acetone/n-hexane and acetone-dichloromethane binary mixtures and single vapors.

For the next phase of the project, several objectives have been formulated.

- 1) Continuation of binary vapor adsorption studies on acetone/hexane and acetone/ CH_2Cl_2 binary mixtures.
- 2) Additional experimental studies on strongly polar-strongly polar binary mixtures adsorbed on BPL-activated carbon.
- 3) Verification of the kinetic saturation capacity (W_e) obtained by the Wheeler equation. W_e should be independent of bed weight. This will be evaluated by conducting studies on a wider range of bed weight. Experiments such as these may shed light on the observation of high W_e values in some systems.

LITERATURE CITED

1. M. M. Dubinin, "Physical Adsorption of Gases and Vapors in Micropores", Progress in Surface and Membrane Science 9, (1975) 1.
2. P. J. Reucroft, W. H. Simpson, and L. A. Jonas, "Sorption Properties of Activated Carbon", J. Phys. Chem. 75, (1971) 3526.
3. C. T. Chiou and P. J. Reucroft, "Adsorption of Phosgene and Chloroform by Activated and Impregnated Carbons", Carbon 15, (1977) 49.
4. P. J. Reucroft and C. T. Chiou, "Adsorption of Cyanogen Chloride and Hydrogen Cyanide by Activated and Impregnated Carbons", Carbon 15, (1977) 2825.
5. L. A. Jonas, "Gas Adsorption Kinetics", Ph.D. Dissertation, University of Maryland (1970).
6. L. A. Jonas and W. J. Svirbely, "Kinetics of Adsorption of CCl_4 and CHCl_3 from Air Mixtures by Activated Carbon", J. Catalysis 24, (1972) 446.
7. L. A. Jonas and J. A. Rehrmann, "Predictive Equations in Gas Adsorption Kinetics", Carbon 11, (1973) 59.
8. P. T. John, V. G. Getty and K. K. Datta, "Microporous Volumes of Carbons by Means of A New Isotherm Equation", Carbon 15, (1977) 169.
9. A. L. Myers and J. M. Prausnitz, "Thermodynamics of Mixed-Gas Adsorption", A.I.Ch.E. J. 11, (1965) 121.
10. L. A. Jonas, E. B. Sansome, and T. B. Farris, "Prediction of Activated Carbon Performance for Binary Vapor Mixtures", Am. Ind. Hyg. Assoc. J., 44, (1983) 716.
11. B. P. Bering, V. V. Serpinsky, and S. I. Surinova, "Mixed Gas Adsorption by Activated Carbons", Dokl. Akad. Nauk. SSSR 153, (1963) 129.

12. B. P. Bering, V. V. Serpinsky, and S. I. Surinova, "Joint Adsorption of a Binary Mixture of Vapors on Activated Charcoal", J. Phys. Chem. (1965) 753.
13. O. R. Quayle, "Precalculation of Equilibrium Parameters of a Binary Mixture of Vapors with Unlimited Solubility in the Liquid State", Chem. Rev. 53, (1953) 439.
14. B. P. Bering, V. V. Serpinsky, and S. I. Surinova, "Substantiation of the Method of an 'Ideal Adsorption Solution' for Calculating the Adsorption of Binary Vapor Mixtures from the Individual Isotherms", J. Physical Chem. (1972) 158.
15. W. K. Lewis, E. R. Gilliland, B. Chertow, and W. P. Cadogen, "Adsorption Equilibria, Hydrocarbon Gas Mixtures", Ind. Eng. Chem. 42, (1950) 1319.
16. R. J. Grant and M. Manes, "Adsorption of Binary Hydrocarbon Gas Mixtures on Activated Carbon", I and EC (Fund.) 5, (1966) 490.
17. A. L. Myers, "Adsorption Gas Mixtures, A Thermodynamic Approach", Ind. Eng. Chem. 60, (1968) 45.
18. A. Wheeler and A. J. Robell, "Performance of Fixed-Bed Catalytic Reactors with Poison in the Feed", J. Catalysis, 13 (1969) 299.
19. A. Wheeler, "Advances in Catalysis", Vol. III, Rheinhold Publishing Company, New York, NY (1951).
20. P. J. Reucroft, R. B. Read, S. Nandy, and P. G. Thoppae, University of Kentucky. First Annual Report. Contract No. DAAK11-82-K-0016, "Modeling of Equilibrium Gas Adsorption for Multicomponent Vapor Mixtures". August 1983. UNCLASSIFIED Report.

21. P. J. Reucroft, K. B. Patel, W. C. Russell, and R. Sekhar, University of Kentucky. Second Annual Report. Contract No. DAAK11-82-K-0016, "Modeling of Equilibrium Gas Adsorption for Multicomponent Vapor Mixtures". August 1984. UNCLASSIFIED Report.

END

1-87

DTIC